AD_____

Award Number: DAMD17-02-1-0712

TITLE: Skin Bioengineering: Noninvasive Transdermal Monitoring

PRINCIPAL INVESTIGATOR: Richard H. Guy, Ph.D.

CONTRACTING ORGANIZATION: University of Geneva, School of Pharmacy
CH-1211 Geneva 4
Switzerland

REPORT DATE: January 2004

TYPE OF REPORT: Annual

PREPARED FOR: U.S. Army Medical Research and Materiel Command
Fort Detrick, Maryland 21702-5012

REPORT DOCUMENTATION PAGE

Form Approved
OMB No. 074-0188

1. AGENCY USE ONLY (Leave blank)	2. REPORT DATE	3. REPORT TYPE AND DATES COVERED
	January 2004	Annual (1 Jan 2003 - 31 Dec 2003)

4. TITLE AND SUBTITLE
Skin Bioengineering: Noninvasive Transdermal Monitoring

5. FUNDING NUMBERS
DAMD17-02-1-0712

6. AUTHOR(S)
Richard H. Guy, Ph.D.

7. PERFORMING ORGANIZATION NAME(S) AND ADDRESS(ES)
University of Geneva, School of Pharmacy
CH-1211 Geneva 4
Switzerland

E-Mail: richard.guy@pharm.unige.ch

8. PERFORMING ORGANIZATION REPORT NUMBER

9. SPONSORING / MONITORING AGENCY NAME(S) AND ADDRESS(ES)
U.S. Army Medical Research and Materiel Command
Fort Detrick, Maryland 21702-5012

10. SPONSORING / MONITORING AGENCY REPORT NUMBER

11. SUPPLEMENTARY NOTES

12a. DISTRIBUTION / AVAILABILITY STATEMENT
Approved for Public Release; Distribution Unlimited

12b. DISTRIBUTION CODE

13. ABSTRACT (Maximum 200 Words)

The long-term objective is to develop and optimize a novel, noninvasive iontophoretic approach for metabolic monitoring via the skin. The low-level current density drives both charged and highly polar (yet neutral) compounds across the skin at rates much greater than passive diffusion. As the skin offers a uniquely accessible body surface across which information can be extracted, we hypothesize that truly noninvasive and highly sensitive devices, which exploit uniquely paired flows of at least two substances, can be developed for iontophoretic monitoring applications. Proof-of-principle targets two analytes of significant interest; specifically, glucose, and lactate.

14. SUBJECT TERMS	15. NUMBER OF PAGES
No Subject Terms.	54
	16. PRICE CODE

17. SECURITY CLASSIFICATION OF REPORT	18. SECURITY CLASSIFICATION OF THIS PAGE	19. SECURITY CLASSIFICATION OF ABSTRACT	20. LIMITATION OF ABSTRACT
Unclassified	Unclassified	Unclassified	Unlimited

Table of Contents

SKIN BIOENGINEERING: NONINVASIVE TRANSDERMAL MONITORING

Richard H. Guy, University of Geneva, School of Pharmacy, Switzerland

Introduction

The long-term objective is to develop and optimize a novel, noninvasive, iontophoretic approach for metabolic monitoring via the skin. The low-level current density drives both charged and highly polar (yet neutral) compounds across the skin at rates much greater than passive diffusion. As the skin offers a uniquely accessible body surface across which information can be extracted, we hypothesize that truly noninvasive and highly sensitive devices, which exploit uniquely paired flows of at least two substances, can be developed for iontophoretic monitoring applications. The research strategy will optimize iontophoretic and sensing technology to satisfy three key criteria for success: (a) fundamental understanding of electrotransport across the skin; (b) reproducible enhancement of transdermal permeability to identify metabolic monitoring opportunities via the skin; and (c) characterization and validation of simple, user-friendly devices for sample collection coupled with sensitive and specific analytical tools. The specific aims of the project are:- {1} To refine understanding of electrotransport across the skin; to exploit the interactions (and independence) of solute and ion flows in the presence of an applied electric field. {2} To demonstrate that the simultaneous, 'reverse iontophoretic' extraction of a target analyte, together with an endogenous substance of essentially constant concentration within the body, can offer truly noninvasive, metabolic monitoring. {3} To engineer simple, elegant, prototypical devices, of small volume (100 μL or less), into which reverse iontophoretically extracted samples may be efficiently collected. {4} To couple these systems to highly sensitive and specific chromatographic and electrochemical analytical tools both off-line and, eventually, on-line, in situ. Proof-of-principle targets two analytes of significant interest; specifically, glucose and lactate. Furthermore, the bioengineering and analytical chemistry advances envisaged will allow broad, 'mass-screening' of the substances extracted (and extractable) by reverse iontophoresis revealing additional opportunities for the approach. In summary, this project aims to evaluate iontophoretic bioengineering technology *in vivo* in man; specifically, applications with respect to metabolic monitoring are foreseen.

Body

The accomplishments of this work since the last report are presented in detail in the following pages. Specifically, three key activities have been achieved: (i) the completion of a manuscript, to be submitted shortly to *Clinical Chemistry*, detailing the application of the internal standard concept to the *in vivo* monitoring, by reverse iontophoresis, of blood sugar; (ii) the development of a method to detect glucose electrochemically, without a mediator, in a polymeric microchip; and (iii) a preliminary proof-of-concept demonstration that reverse iontophoresis can be applied to the noninvasive monitoring of lactate.

Non-invasive glucose monitoring by reverse iontophoresis in vivo: Application of the internal standard concept

Anke Sieg[1,2], Richard H.Guy[1,2], M.Begoña Delgado-Charro[1,2*]

[1]University of Geneva, School of Pharmacy, Quai Ernest-Ansermet 30, CH-1211 Geneva, Switzerland

[2]Centre interuniversitaire de recherche et d'enseignement, "Pharmapeptides", Campus universitaire, Parc d'affaires international, F-74160 Archamps, France

*Corresponding author. Tel. +33 450 315022
Fax: +33 450 95 28 32
email: Begonia.Delgado@pharm.unige.ch

source of support: grants, etc.: see covering letter

Keywords:

Skin, Transdermal, Iontophoresis, Glucose monitoring, Electroosmosis

Abbreviations:

J	Iontophoretic flux
A	Analyte
IS	Internal Standard
K	Constant for iontophoretic extraction
Ph.Eur.	Pharmacopoeia Europea

Abstract:

Background:

The GlucoWatch Biographer uses reverse iontophoresis to extract glucose across the skin to monitor glycemia in diabetes. The invasive daily calibration with a conventional "fingerstick" has been perceived as disadvantage. Here, an "internal standard" is used so as to render the approach completely non-invasive.

Methods:

The simultaneous extraction of glucose and sodium by reverse iontophoresis was performed on human volunteers over 5 hours, and blood glucose was measured in the conventional manner at each collection interval. These data were used for each subject to calculate an extraction constant (K), which equals the ratio of the extracted fluxes (J_{glc}/J_{Na+}) normalized by the corresponding ratio of the concentrations in the blood ([glu]/[Na^+]). The values of K were compared between and within subjects.

Results:

The iontophoretically extracted glucose flux reflected the glucose concentration profiles in the blood, sodium extraction remained essentially constant consistent with the fact that its systemic concentration does not vary significantly. A constant value of K was established for part of the study population, therefore, allowing for an accurate prediction of glycemia without the need for a calibrating blood sample. However, further experimentation in additional subjects revealed seasonal changes in the efficiency of glucose extraction, that were not mirrored by the reverse iontophoresis of Na^+. That is, variation in K became apparent.

Conclusions:

The "internal standard" should be useful for the determination of glycemia by reverse iontophoresis without calibrating with a blood sample. While Na^+ can be a useful internal standard, this research demonstrates that a neutral molecule, extracted by the same mechanism as glucose, would represent a better alternative.

Introduction:

New techniques that measure analytes in the body non-invasively are subject of considerable interest. The monitoring of blood sugar, in particular, is of great importance because of the large and growing population of diabetics who require regular and accurate information about their glucose levels. The Diabetes Control and Complications Trial confirmed that blood glucose control can efficiently reduce the long-term complications of diabetes (1). Conventional self-testing methods require a blood sample, typically from the fingertip, a painful and inconvenient procedure with poor patient compliance. Consequently, there is considerable investment of resources at present in the development of non-invasive and continuous glucose monitoring technologies (2).

One such approach is iontophoresis, which uses a small electric current to drive charged and highly polar compounds across the skin at rates very much greater than their passive permeabilities. Two major transport mechanisms are involved: electromigration and electroosmosis. Electromigration is the movement of small ions across the skin under the direct influence of the electric field. Electron fluxes are transformed into ionic fluxes via the electrode reactions, and ionic transport proceeds through the skin to maintain electroneutrality. The total charge transported depends on the strength of the electric field and the duration of application. Iontophoresis sets in motion a number of ions across the skin, and all of them compete to carry a fraction of the current. The contribution of each ion to charge transport is called the transport number, the sum of which equals 1. According to Faraday's law, the flux of each ion in the iontophoretic circuit is given by:

$$J_i = (t_i * I)/(F * z_i) \qquad \text{(Equation 1)}$$

where J_i^1 is the flux of the ith ion, t_i is its transport number, and z_i is the valence; F is Faraday's constant and I is the total current flowing. Transport numbers depend on the relative mobility and concentration of all mobile ions in the iontophoretic system and, given that sodium chloride is the principal extracellular electrolyte in the body, Na^+ and Cl^- carry a major fraction of the current in iontophoresis.

Electroosmosis is the principal transport mechanism of uncharged molecules and of high molecular weight cations. The skin is negatively charged at physiological pH and acts, therefore, as a permselective membrane to cations. This preferential passage of counterions induces an electroosmotic solvent flow that may carry neutral molecules in the anode-to-cathode direction. The volume flow J_V (volume*time^{-1}*area^{-1}) is predicted (3) to be proportional to the potential gradient ($-d\Phi/dx$) established by the electric field:

$J_v = L_{VE} * (-d\Phi/dx)$ (Equation 2)

where L_{VE} is the electroosmotic flow coefficient describing the direction and the magnitude of the volume flow. The molar flux of a solute "j" present at a molar concentration c_j is then:

$J_j = J_V * c_j$ (Equation 3)

Electroosmosis depends on the charge on the membrane and may be modified by solutions (e.g., their pH) which "couple" the electrodes to the skin, thereby changing the value of L_{VE}.

In clinical chemistry, iontophoresis has already been established as a tool used in the diagnosis of cystic fibrosis (whereby pilocarpine is administered to test the secretional function of the sweat glands)(4). The symmetry of iontophoresis renders it useful, not only for the delivery of drugs, but also for the extraction of endogenous substance of clinical interest and, in particular, glucose (5).

This latter application has been investigated in depth and has led to the development of the GlucoWatch® Biographer (Cygnus Inc., Redwood City, CA) (6)-(10). The wrist-worn device monitors glucose continuously for up to 13 hours, recording six glucose readings per hour. However, the device needs to be calibrated against blood glucose from the fingertip to correlate the extracted glucose amounts with subdermal levels. This essential step has been perceived as disadvantage despite the fact that the GlucoWatch provides tremendously more information to the diabetic than (the normal) one or two "finger-sticks" per day. A completely non-invasive calibration approach would therefore be beneficial and would open the way to other applications of the reverse iontophoresis technology.

The concept addressed here is that of an internal standard (11). As iontophoresis is nonspecific, many ions and small uncharged species (in addition to the analyte of interest) are moved across the skin by the applied electric field. Instead of detecting uniquely the single, target substance and calibrating its transdermal measurement via a blood assay, the idea is to monitor the extraction of two species simultaneously: the compound of interest, the temporal change in whose concentration is of clinical importance (i.e. glucose), and a second analyte, the physiological concentration is known and essentially fixed. If the iontophoretic transport of the analyte (A) and the latter, "internal standard" (IS), are independent of one another, then their fluxes (J) out of the skin should obey the relationship:

$J_A/J_{IS} = K * [A]/[IS]$ (Equation 4)

where [A] and [IS] are the blood concentrations of the two substances, and K is a constant. The sodium ion, being a major charge carrier in the anode-to-cathode-direction, was selected

as a potential internal standard. Previously, we have shown *in vitro* (11) That the relationship in Equation 4 is obeyed even when the subdermal [Na^+] was allowed to vary over its maximum physiological range (125-145 mM).

The aim of the research described here is to test the internal standard hypothesis *in vivo*. The following questions were addressed: (a) what is the flux ratio J_{glc}/J_{Na+} *in vivo*, (b) can a common proportionality constant K be established for a subject population, (c) how accurate is the prediction of blood glucose when using the "internal standard" concept, and (d) what is the significance of inter- and intra-individual variability with respect to iontophoretic extraction? In addition, the potential utility of potassium as another cationic internal standard was examined.

Materials and Methods

Study population

14 non-diabetic subjects (aged from 25 to 39 years; 4 males, 10 females), with no history of skin diseases participated in the study. Informed consent had been obtained, the study protocol having been approved by the internal review board of the University of Geneva in accord with the principles outlined in the Declaration of Helsinki. In total, 42 experiments were performed: 8 subjects participated on a single occasion, while 6 volunteers participated two and more frequently.

Chemicals

Tris base (α,α,α-Tris-(hydroxymethyl)-methylamine), sodium chloride, potassium chloride, D-glucose, hydrochloric acid, sodium hydroxide, and methanesulfonic acid were purchased from Sigma-Aldrich Co. (St. Quentin Fallavier, France) and were at least of analytical grade. Deionized water (resistivity > 18.2 Mohm/cm^2) was used to prepare all solutions.

Iontophoresis

Two cylindrical glass cells (diameter 1.6 cm, extraction surface 2 cm^2) were fixed with foam tape (3M, Health Care, St. Paul, MN) on the subjects' ventral forearm with a

distance of 7 cm between them. The anodal chamber was filled with 1.2 ml of 10 mM Tris-buffer at pH 8.5 containing 100 mM NaCl; the cathodal chamber contained the same volume of 10 mM Tris buffer alone. Custom-made Ag/AgCl electrodes were inserted into the solutions and fixed 3-4 mm above the skin surface to ensure that no physical contact with the skin occurred. Direct current (I=0.6 mA, current density = 0.3 mA/cm^2) was passed for a total of 5 hours and was controlled by a Phoresor II Auto (Iomed, Salt Lake City,UT), an FDA-approved, constant current, iontophoretic power supply. Every 15 minutes post-initiation of the current, the entire cathodal solution was collected and replaced by 1.2 ml of fresh buffer. The samples were immediately frozen until analysis.

After 2 hours of iontophoresis, the subjects ingested either (a) a meal rich in carbohydrates, or (b) 75g of glucose dissolved in 300 ml of water (Glucosum monohydricum Ph.Eur., Hänserler AG, Herisau, Switzerland), so as to provoke a significant change in blood sugar. From this point onwards, glycemia was measured before each subsequent 15-minute collection interval using a conventional blood glucose monitor (Glucotrend 2, Roche Diagnostics, Mannheim, Germany). The "within-run" and "day-to-day" imprecision of the glucose monitor was ≤ 3%, the accuracy against an automated hexokinase reference method was y[mmol/l] = 0.08 + 0.98x (information from the supplier).

Analytical chemistry

Analytes were separately assayed by high-performance ion chromatography on a Dionex Ion chromatograph 600 system (Dionex, Sunnydale, CA). Glucose was quantified by anion-separation with pulsed amperometric detection on a gold electrode; Na^+ and K^+ were quantified by cation-separation with suppressed conductivity detection. Calibration was performed with at least 6 external standards in each chromatographic run, covering a linear range ($r^2 \geq 0.999$) for glucose between 0 and 30 µM, Na^+ 0 - 5 mM, K^+ 0 - 1 mM. The limits of quantification (expressed as 10-fold signal-noise-ratio) for glucose, Na^+ and K^+ were 0.15 µM, 1.4 µM, and 2.5 µM, respectively. The "within-run" variability of injection was 2.1% for a mean concentration of the analytes.

Data analysis and statistics

Iontophoretic fluxes were calculated from the amounts extracted in each collection interval and plotted at the mid-time point of each interval, blood glucose concentrations were at the actual time of measurement.

Data are expressed as mean ± standard deviation (SD). Average Na^+ fluxes were in each experiment determined from 12 separate points. Electroosmotic volume flows were determined by normalizing the reverse iontophoretic flux values by the corresponding blood concentrations; according to Equation 3. Statistical differences were assessed by two-tailed Student's t-test and ANOVA, followed by a Newman-Keuls Multiple Comparison Test, using GraphPad Prizm 3.02 software (San Diego, CA). Individual values of K were determined by linear regression, for which significance was tested by ANOVA. A common value of K was computed by pooled regression based on six experiments from different volunteers using analysis of covariance as described in (12). The accuracy of prediction was tested by plotting the predicted glucose values against the measured blood glucose in a Clark Error Grid (13).

Results and discussion

Local effects of iontophoresis

All subjects experienced a mild tingling sensation when the current was applied. The sensation was typically asymmetric, with more tingling felt at the anode than at the cathode. Generally, the sensation diminished with time of current application and lasted no longer than 30 minutes. Iontophoresis caused the skin sites beneath the electrode chambers to become slightly erythematous, an effect which disappeared within 24 hours. In addition, a few, small, punctuate lesions remained after the redness disappeared; these marks persisted for several days. These completely reversible effects are similar to those that have been reported in the literature (7), are and do not appear to impair skin barrier function. In two subjects, after 60 minutes of current application, small blisters were seen beneath the electrode chambers and the experiment was interrupted. The blisters subsequently diminished in size and disappeared completely within a few hours. It is believed that hypersensitivity to Tris buffer caused this reaction. The two subjects were excluded from further study.

Commentaire : ref

Glucose tracking

The iontophoretic transport of glucose, an uncharged, polar molecule, occurs by electroosmosis and is directly proportional to the subdermal concentration (3). However, a "warm-up" period is necessary to establish a pseudo-steady electroosmotic flow and to empty the glucose reservoir from the skin. The latter is due to local metabolism and is not reflective of glucose levels in the blood. The recommended "warm-up" period for the GlucoWatch G2

is two hours, a peroid similarly adopted in this study. Subsequently, extraction every 15 minutes over the next 3 hours allowed blood glucose tracking in 8 of the 12 subjects studied. In these volunteers, electroosmotic flow was greater than 5 $\mu l*h^{-1}$ (Table 1). Figure 1 shows the glucose extraction profiles for 3 volunteers who ingested on separate occasions either a carbohydrate-rich meal, or 75g of a standard glucose load, at 150 minutes. The glucose reverse iontophoretic extraction fluxes followed accurately the systemic glucose concentration. A time delay between the extraction rate and the blood level was apparent in those subjects receiving the oral glucose load. Rapid absorption of glucose occurred with a higher peak value obtained (14mM versus 10mM) relative to those subjects who received a carbohydrate-rich meal. In contrast, ingestion of the carbohydrate rich meal resulted in a more gradual glucose absorption from the gastrointestinal tract such that differences between the plasma kinetics and the rate of extraction were blurred.

It is acknowledged that reverse iontophoresis samples the interstitial fluid and that real differences exist between glucose kinetics in this compartment and those in the blood; this divergence is clearly relevant to the development of continuous glucose monitoring devices and the site(s) at which glucose is determined. For example, Réach at el. (14) have described a delayed response between increasing glucose levels in the interstitium as compared to those in the blood in rats. On the other hand, a faster and more pronounced decrease of glucose in the interstitium was observed when blood sugar was lowered. This physiological lag (estimated to be somewhat less than 4 minutes) was similarly observed in humans using the GlucoWatch (15). The possibility that insulin increases skin blood flow has also been reported (16) and this, in turn, might influence glucose extraction by reverse iontophoresis.

The "warm-up" period of 2 hours iontophoresis was sufficient to establish pseudo-steady electroosmosis. However, in subject 6 (see Figures 1A and 1B), an additional 45 minutes was necessary before glucose fluxes stabilized; from this point, good tracking of glycemia was observed.

Generally speaking, accurate glucose measurements by iontophoresis required efficient extraction. Only moderate or poor correlation was found when the normalized glucose fluxes were lower than 5 $\mu l*h^{-1}$; above this threshold, however, good to excellent agreement was obtained.

Cation extraction

Reverse iontophoretic extraction fluxes of sodium are shown in Table 1 for all subjects. These values stabilized 30 minutes after the initiation of iontophoresis (not shown) and remained essentially constant throughout the experiments even when significant changes in glycemia were occuring (see Figure 1). The calculated average transport number of sodium in these experiments was 0.55 ± 0.4. This is consistent with the *in vitro* results (11) and demonstrates that Na^+ is the principal charge carrier across the skin. Given that Na^+ is present in the body at levels 30 to 50 times higher than other potential charge carriers such as K^+, Ca^{2+} or Mg^{2+}, this result is not surprising. At this high concentration, Na^+ iontophoresis is effectively independent of its subdermal concentration over the physiological range of 125 to 145 mM and is unlikely to be affected by changes in the plasma level of the other cations. Thus, alterations in the systemic Na^+ concentration during hypo- or hyperglycemia were not anticipated to affect the utility of Na^+ as an internal standard. The results from this study support this assumption in that reverse iontophoretic extraction of Na^+ was remarkably constant wihtin and between subjects and was not significantly altered even whenlarge excursions in glycemia occurred (see Figure 1).

Potassium fluxes varied between subjects and within the same experiment (data not shown), being higher at the beginning of iontophoresis before gradually decreasing after two hours of iontophoresis to values between 0.7 and 3.9 $\mu mol*h^{-1}$; the calculated average transport number was 0.07 ± 0.04, corresponding to a coefficient of variation more than ten times greater than that for sodium transport. Interestingly, the highest potassium fluxes were found in subjects with the lowest electroosmotic flux, an observation that needs to be confirmed in a larger population and the reason for which (if real) is unclear. The higher variability and lower transport number of potassium precluded its use for the calibration of glucose extraction and no further work was pursued.

Common extraction constant (K)

The ratio of subdermal concentrations of glucose and Na^+ (assumed to be 133 mM) were calculated and plotted against the corresponding ratio of extracted fluxes (Figure 2). Linear regression (see Equation 4) for each subject yielded an individual value of K, given in Table 1. These data are from 6 subjects, for whom the normalized glucose flux was ≥ 8.5 $\mu l*h^{-1}$, and were used to determine an average value of K. Analysis of covariance showed no

significant difference the indidividual K values. Pooled ANOVA yielded a common slope, that is, the common average extraction constant, namely 0.12 ± 0.018.

Prediction of blood glucose

The average K can be used to estimate blood glucose from the iontophoretic extraction flux data, via the rearrangement of equation 4:

$$[\text{Glucose}] = (J_{\text{Glucose}}/J_{\text{Na+}}) * ([Na^+]/K) \qquad \text{(Equation 5)}$$

Data from a further 16 experiments, in which electroosmosis was again $\geq 8.5\ \mu l*h^{-1}$, were analyzed in this way and the estimated blood glucose concentrations were then compared to glycemia measured from the fingertip. The results, plotted as a Clark Error Grid, are shown in Figure 3. Of a total of 181 data points, 142 (78.5%) fell in region A, 39 (21.5%) fell in region B; that is, all results were in the clinical acceptable region A+B. It must be accepted, however, that the range of glycemia covered by these experiments was limited: 4 – 13 mM. Additional work is necessary to determine whether the predictions remain robust at more extreme levels of hypo- and hyperglycemia. Linear correlation through all the data points in Figure 3 yielded a slope of 0.96 ± 0.05 and an intercept of 0.10 ± 0.36. The correlation coefficient was 0.80.

Inter- and intra-individual variability

Glucose fluxes differed significantly in subjects 6 to 9 from the rest of the population (see Table 1). Electroosmotic glucose transport was approximately an order of magnitude lower than that seen in the other subjects. In contrast, essentially no differences in sodium extraction were found, with all values falling in the range of 10.7 to 13.3 $\mu mol*h^{-1}$. This contrast is visualized in Figure 4. As a result, the K values for subjects 6 – 9 were clearly smaller (Table 1) and the use of the previously discussed common K value would not yield accurate predictions of glycemia in these volunteers.

It might then be argued at this point, instead of attempting to use a common K for all subjects, that K be determined for each individual in a separate calibration experiment. However, such an approach also demands that the within-subject variability as a function of time is reasonable. To test this hypothesis, monthly experiments were performed on subject 1 over the course of a calendar year. The results for the nomalized glucose flux and the iontophoretic Na^+ extraction kinetics are in Figure 5. While Na^+ transport remained constant, significant decreases in electroosmosis were observed in the winter month. Additional data were also acquired in other subjects (see Table 2) and revealed no clear pattern. Subjects 2

and 10 behaved simimarly to subject 1 while two other volunteers (3 and 4) showed no seasonal effect; subject 6, in contrast, manifested a lower electroosmotic flow in the summer. In only two subjects (4 and 10) were Na^+ fluxes significantly different, although the disparities would not have practical importance. Taken together, therefore, it appears that even an individual calibration for each subject might not permit an accurate prediction of glycemia at all times via the "internal standard" approach.

While the fundamental reason for the variability in glucose extraction cannot be unequivocally deduced from this work, it can be concluded that a more appropriate internal standard will probably be another neutral substance that is transported by the same electroosmotic mechanism. In this way, any effects which change the charge on the skin (and/or its permselectivity) will similarly alter the extraction of glucose and the internal standard. The sodium ion, on the other hand, as the major charge carrier across the skin is not very sensitive to relatively subtle differences in skin charge. As such, it is a less than ideal internal standard for glucose. On the other hand, recent work has demonstrated the very appropriate use of Na^+ as an internal standard for the use of reverse iontophoresis as a non-invasive tool in the therapeutic monitoring of lithium. In this case, the normalization of lithium extraction flux with that of Na^+ resulted in an improved prediction of the drug's serum level in bipolar patients *in vivo* (17).

Comparison with in vitro data

The average K measured in this work is somewhat higher than that measured *in vitro* with porcine skin; in that study mean electroosmotic flow of 5.1 $\mu l*h^{-1}$ together with an average sodium flux of 8.0 $\mu mol*h^{-1}$ gave a constant of 0.07(11). Two factors, at least may contribute to the better extraction *in vivo*: (I) the electrode formulations were modified to maximize as far as possible the electroosmotic flow (e.g., pH 8.5 was used), and (ii) the presence of a functioning microcirculation provides for more facile access to the subdermal compartment. Particularly interesting, however, is that the marked variability in glucose extraction *in vivo* was not observed *in vitro*. At pH 7.4, electroosmosis varied no more than 30% and a seasonal difference was not observed. A possible explanation may lie in the physiology of the skin appendages (e.g., the sweat glands) which have been recognized as important transport pathways in iontophoresis (18). Inter-individual differences in appendageal morphology and effects of climate on function have been reported (19),(20), and may account for the greater variation observed *in vivo*, as a function of ambient conditions. Additional work is clearly needed to better understand these observations.

Conclusion

The study demonstrates the development of the reverse iontophoresis approach to monitor glucose non-invasively without calibration with a blood sample. The "internal standard" hypothesis, using Na^+ ion as the invariant endogenous calibrator, was confirmed for a subset of the study population. However, Na^+ , being extracted by a different mechanism than glucose, did not reflect the entire range of variability in glucose extraction. It follows that, for glucose monitoring, the ideal internal standard would be another uncharged compound (whose blood concentration is known and essentially invariant) of similar physicochemical properties).

Acknowledgements

This work was supported by the "Programme commune de recherche en génie biomédical" of the EPFL and the Universities of Lausanne and Geneva, Switzerland, and by USAMRAA grant DAMD17-02-1-0712 (Fort Detrick, MD),and by the US National Institute of Health (EB 001420) The information presented does not necessarily reflect the position or the policy of the U.S. Government, and no official endorsement should be inferred.

References

(1) The Diabetes Control and Complications Trial Research Group. The effect of intensive treatment of diabetes on the development and progression of long-term complications in insulin-dependent diabetes-mellitus. N Engl J Med 1993;329:977-86

(2) Koschinsky T, Heinemann L. Sensors for glucose monitoring: technical and clinical aspects. Diabetes Metab Res Rev 2001;17:113-123

(3) Pikal JM. The role of electroosmotic flow in transdermal iontophoresis. Adv Drug Del Rev 1992;9:201-237

(4) Webster HL. Laboratory diagnosis of cystic fibrosis. Crit Rev Clin Lab Sci 1983;18:313-338

(5) Guy RH. Iontophoresis - Recent developments. J Pharm Pharmacol 1998;50:371-374

(6) Rao G, Glikfeld P, Guy RH. Reverse iontophoresis: development of a non- invasive approach for glucose monitoring. Pharm Res 1993;10:1711-1715

(7) Rao G, Guy RH, Glikfeld P, LaCourse WR, Leung L, Tamada J, Potts RO, Azimi N. Reverse iontophoresis: non-invasive glucose monitoring in vivo in humans. Pharm Res 1995;12:1869-1873

(8) Tamada JA, Bohannon NJV, Potts RO. Measurement of glucose in diabetics subjects using non-invasive transdermal extraction. Nature Med 1995;1:1198-1201

(9) Tierney MJ, Tamada JA, Potts RO, Eastman RC, Pitzer KR, Ackerman NR, Fermi S. The GlucoWatch biographer: a frequent automatic and noninvasive glucose monitor. Ann Med 2000;32:632-641

(10) Eastman RC, Chase HP, Buckingham B, Hathout EH, Feller-Byk L, Leptien A, et al. Use of the GlucoWatch Biographer in children and adoslescents with diabetes. Pediatric Diabetes 2002;3:127-134

(11) Sieg A, Guy RH, Delgado-Charro MB. Reverse Iontophoresis for Noninvasive Glucose Monitoring: The Internal Standard Concept. J Pharm Sci 2003;92:2295-2302

(12) Zar JH. Biostatistical Analysis, 2nd ed. Englewood Cliffs: Prentice-Hall, 1984:718pp.

(13) Clark WL, Cox D, Gonder-Frederik LA, Carter W, Pohl SL. Evaluating Clinical Accuracy of Systems for Self-Monitoring of Blood Glucose. Diabetes Care 1987;10:622-8.

(14) Aussedat B, Dupire-Angel M, Gifford R, Klein JC, Wilson GS, Reach G. Interstitial

Commentaire : Page: 5
Another reference? See Cygnus list

glucose concentration and glycemia: implications for continuous subcutaneous glucose monitoring. Am J Physiol (Endocrinol Metab) 2000;278:E716-E728.

(15) Kulcu E, Tamada JA, Reach G, Potts RO, Lesho MJ. Physiological difference between interstitial glucose and blood glucose measured in human subjects. Diabetes Care 2003;26:2405-2409

(16) Serné EH, Ijzerman RG, Gans ROB, Nijveldt R, de Vries G, Evertz R, Donker AJM, Stehouwer CDA. Direct evidence for insulin-induced capillary recruitment in skin of healthy subjects during physiological hyperinsulinemia. Diabetes 2002;51:1515-1522

(17) Leboulanger B, Aubry JM, Bondolfi G, Guy RH, Delgado-Charro. Reverse iontophoretic monitoring of lithium in vivo [Abstract]. Ther Drug Monit 2003;25:499

(18) Cullander C, Guy RH. What are the pathways of iontophoretic current flow through mammalian skin? Adv Drug Deliv Rev 1992;9:119-135

(19) Sato F, Owen M, Matthes R, Sato K, Gisolfi CV. Functional and morphological changes in the eccrine sweat gland with heat acclimation. J Appl Physiol 1990;69:232-236

(20) Sato K, Sato F. Individual variations in structure and function of human eccrine sweat gland. Am J Physiol (Regulatory Integrative Comp Physiol) 1983;245:R203-R208

Table of Figures

Figure 1A:

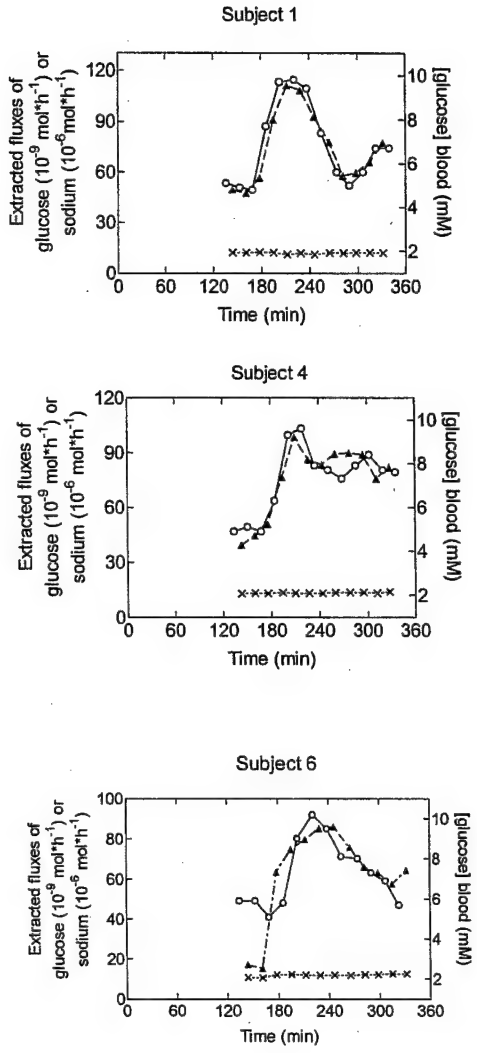
Subject 1
Extracted fluxes of glucose (10^{-9} mol*h^{-1}) or sodium (10^{-6}mol*h^{-1})
[glucose] blood (mM)
Time (min)
Subject 4
Extracted fluxes of glucose (10^{-9} mol*h^{-1}) or sodium (10^{-6} mol*h^{-1})
[glucose] blood (mM)
Time (min)
Subject 6
Extracted fluxes of glucose (10^{-9} mol*h^{-1}) or sodium (10^{-6} mol*h^{-1})
[glucose] blood (mM)
Time (min)

Figure 1B:

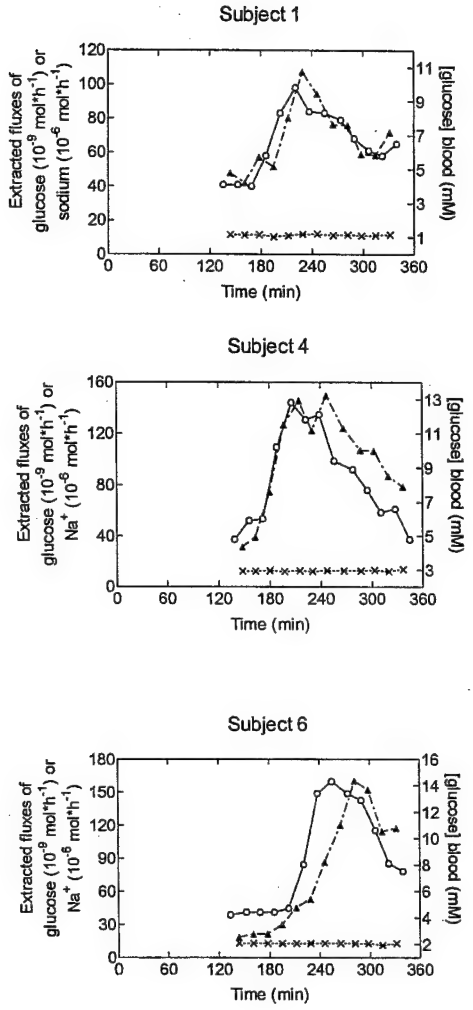
Subject 1
Extracted fluxes of glucose (10^{-9} mol*h^{-1}) or sodium (10^{-6} mol*h^{-1})
[glucose] blood (mM)
Time (min)
Subject 4
Extracted fluxes of glucose (10^{-9} mol*h^{-1}) or Na^+ (10^{-6} mol*h^{-1})
[glucose] blood (mM)
Time (min)
Subject 6
Extracted fluxes of glucose (10^{-9} mol*h^{-1}) or Na^+ (10^{-6} mol*h^{-1})
[glucose] blood (mM)
Time (min)

Figure 2:

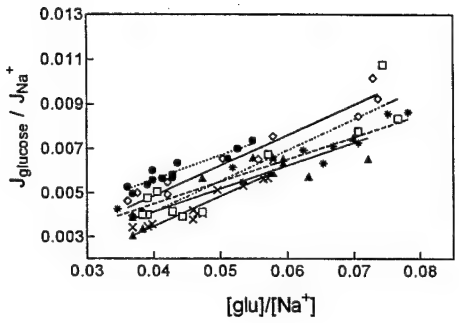

Figure 3:

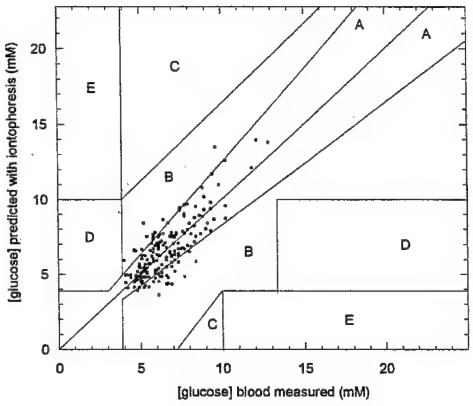

Figure 4:

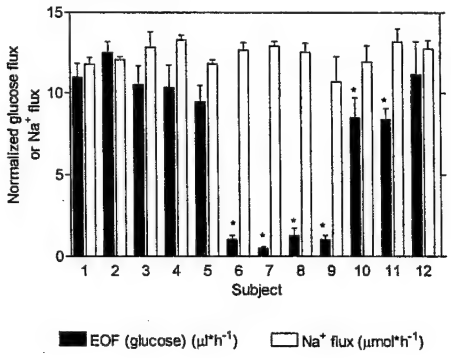

Figure 5:

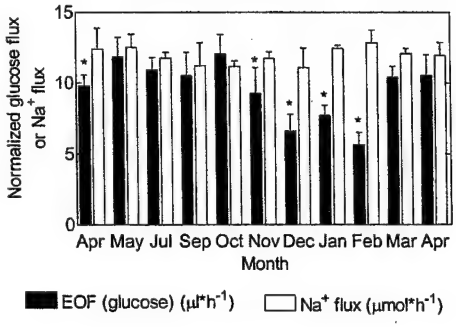

Table 1: Normalized reverse iontophoretic glucose fluxes (with respect to the corresponding blood sugar concentration) and the absolute values of sodium electrotransport in 12 subjects. The constant K was determined from Equation 4.

Subject	Normalized glucose flux ($\mu l*h^{-1}$)	Na^+ flux ($\mu mol*h^{-1}$)	K ± SD	r^2
1	10.9 ± 0.9	11.8 ± 0.4	0.137 ± 0.010[a]	0.95
2	12.5 ± 0.7	12.1 ± 0.2	0.110 ± 0.012[a]	0.90
3	10.5 ± 1.2	12.8 ± 0.9	0.114 ± 0.019[a]	0.85
4	10.3 ± 1.4	13.3 ± 0.3	0.105 ± 0.017[a]	0.80
5	9.4 ± 1.0	11.8 ± 0.3	0.136 ± 0.014[a]	0.90
6	1.1 ± 0.2	12.7 ± 0.5	0.007 ± 0.003	0.47[c]
7	0.5 ± 0.1	12.9 ± 0.3	0.023 ± 0.007	0.53[c]
8	1.3 ± 0.5	12.5 ± 0.6	n.s.[c]	< 0.1[c]
9	1.0 ± 0.2	10.7 ± 1.6	n.s.[c]	< 0.1[c]
10	8.5 ± 1.2	11.9 ± 1.0	0.136 ± 0.014[a]	0.90
11	8.4 ± 0.7	13.2 ± 0.8	0.280 ± 0.108	0.57[b]
12	11.2 ± 2.0	12.7 ± 0.5	n.s.	0.25[b]

[a] Results used to compute the average, population value of K

[b] The poor correlation was due a small variation in blood glucose levels during the experiment. However, data were included in the Clark Error Grid.

[c] Efficiency of glucose extraction was poor, markedly increasing the error in the determination of glycemia from the iontophoretic data (see text). The values of K were not significantly different (n.s.) from zero.

Table 2:

Subject	Season	Normalized glucose flux ($\mu l*h^{-1}$)	Na^+ flux ($\mu mol*h^{-1}$)	K ± SD	r^2
1	S	10.9 ± 0.9	11.8 ± 0.4	0.137 ± 0.010	0.95
	W	6.6 ± 1.2[a**]	11.1 ± 1.4	0.071 ± 0.007	0.91
2	S	12.5 ± 0.7	12.1 ± 0.2	0.110 ± 0.012	0.90
	W	9.0 ± 1.2[a**]	11.7 ± 0.2	0.087 ± 0.021	0.65
3	S	10.5 ± 1.2	12.8 ± 0.9	0.114 ± 0.019	0.85
	W	9.7 ± 1.0	12.5 ± 0.7	0.083 ± 0.009	0.91
4	S	10.3 ± 1.4	13.3 ± 0.3	0.105 ± 0.017	0.80
	W	11.4 ± 2.4	12.5 ± 0.5[a*]	0.140 ± 0.017	0.87
6	S	1.2 ± 0.2	12.7 ± 0.5	0.007 ± 0.003	0.47
	W	8.4 ± 3.3[a**]	12.6 ± 0.5	0.125 ± 0.020	0.79
10	S	8.5 ± 1.2	11.9 ± 1.0	0.136 ± 0.014	0.90
	W	5.2 ± 1.0[a**]	12.6 ± 0.3[a*]	0.029 ± 0.004	0.86

[a] Values measured during the winter (W) were significantly different from those determined in (S) summer value **$p < 0.0001$, *$p < 0.001$

ELECTROCHEMICAL DETECTION OF GLUCOSE WITHOUT MEDIATOR IN A POLYMERIC MICROCHIP

Physical and Analytical Electrochemistry Laboratory, EPFL, Lausanne

1. Introduction

Glucose oxidase catalyses the oxidation of glucose to gluconic acid and hydrogen peroxide (Fig. 1). Its major use is in the determination of free glucose in body fluids. Although specific for (beta)-D-glucose, glucose oxidase can be used to measure total glucose because, as a result of the consumption of (beta)-D-glucose, (alpha)-D-glucose from the equilibrium is converted to the (beta)-form by mutarotation.

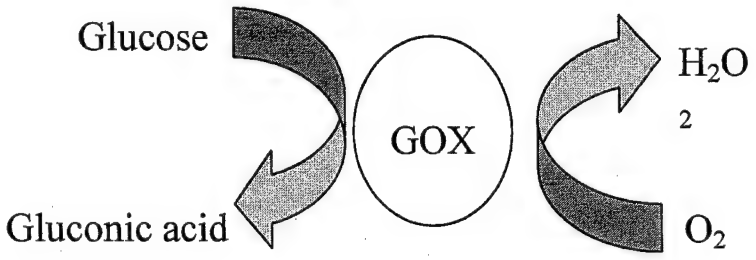

Figure 1: Glucose oxidation by oxygen catalysed by glucose oxidase

2. Experimental

2.1. Chemicals and materials

Gold disk electrode
Polymer microchips with four electrodes in micro-channel (Diagnoswiss)
Electrochemical measurements with a 2-electrode configuration, using Ag/AgCl as reference electrode
Autolab Electrochemical workstation
Glucose
GOx 220U/mg (Fluka)
PBS 10mM pH 7.4 with 140mM NaCl
PB 10mM

3. Set up

First, a calibration of H_2O_2 was achieved with a gold disk electrode as shown in Figure 2a, then in the microchip systems shown in Figure 2b. All the measurements were performed in a Faraday cage.

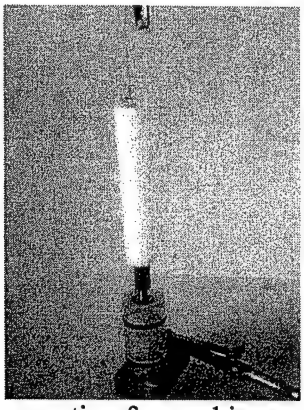

Figure 2a: Electrical connection for working and reference electrodes.

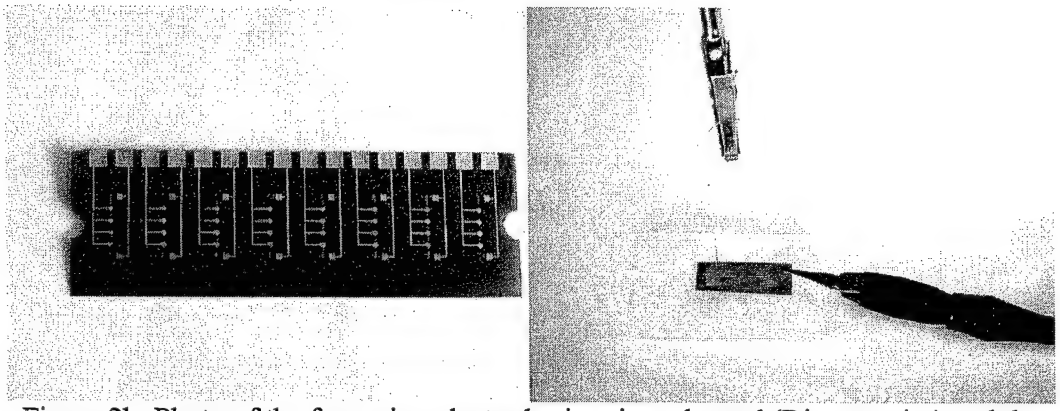

Figure 2b: Photo of the four microelectrodes in micro channel (Diagnoswiss) and the electrical connection.

4. Procedure

4.1 Hydrogen peroxide calibration

Solutions from 0.1 to 25mM H_2O_2 in PBS 10mM.

4.1.1. Gold disk electrode

A drop of 50 µL of H_2O_2 solution was placed on the top of the gold disk electrode, and the reference electrode was inserted. Direct measurement by differential pulse was carried out at least three times for each solution. The working electrode was polished with alumina between each solution.

Differential pulse conditions
Eq. Time : 5s
Mod. Time : 0.05s
Int. Time : 0.5s
Pot in : 0V
Pot end : -1V
Step pot. : 0.0195V/s
Mod. Ampl. : 0.02505V

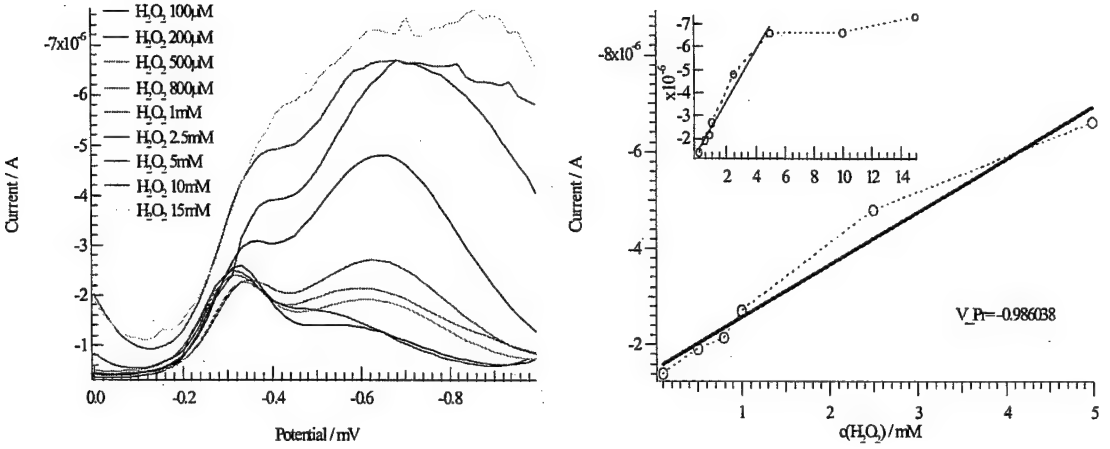

Figure 3: DPV of hydrogen peroxide on gold disk electrode. A plateau is reached at H_2O_2 concentrations higher than 10mM.

4.1.2. H_2O_2 calibration in microchips

A drop of 50 µL was placed on a reservoir and the channel was filled using a vacuum pump. The channel was rinsed with the subsequent concentration of H_2O_2 to be measured. The differential pulse conditions were as before.

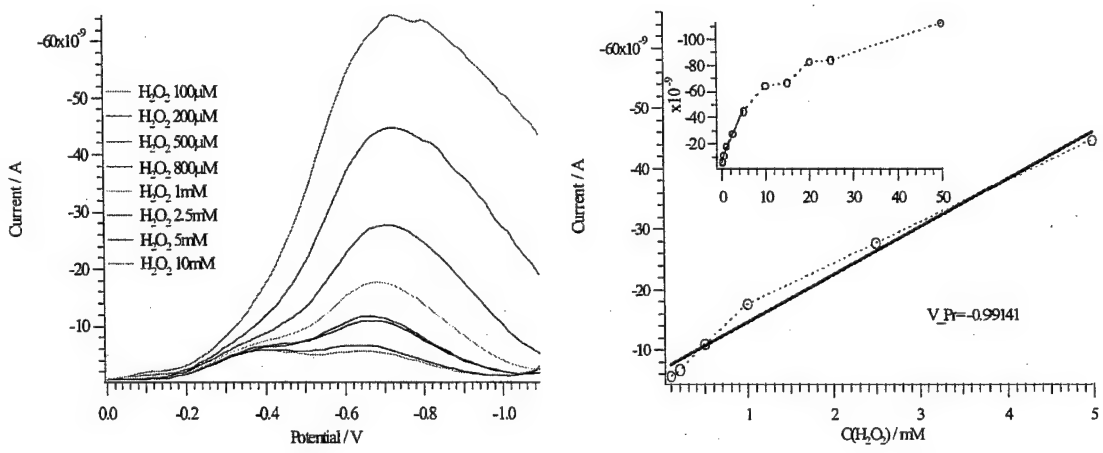

Figure 4: DPV of hydrogen peroxide on gold electrode in microchip. A plateau is reached at H_2O_2 concentrations higher than 10mM

The differential potential response between the gold disk electrode and the gold electrode in microchips could be due to the different electrode materials and/or to the speed of diffusion. The gold electrodes in microchips are copper-coated with a gold film. The potential for the response of the microchips and for that of the gold disk are, respectively: –0.35V for O_2, and –0.65V for H_2O_2; and –0.4V for O_2 and –0.7V for H_2O_2.

4.2. Glucose oxidase adsorption in microchips

4.2.1. GOx adsorption

A solution of 1mg/ml GOx in PBS was prepared. This corresponds to a concentration of 2200U/ml of enzyme. The channel was filled with the GOx solution and the enzyme was allowed to adsorb during 1 hour at room temperature. The channel was then washed with a solution of PBS 10mM. The microchips were dried under vacuum and stored at 4°C.

A solution of glucose in PBS 10mM with a range of 1 to 50mM was first used to determine the limit of sensibility.

The same procedure and conditions as for the hydrogen peroxide calibration were employed. The evolution of H_2O_2 formation was followed as a function of time.

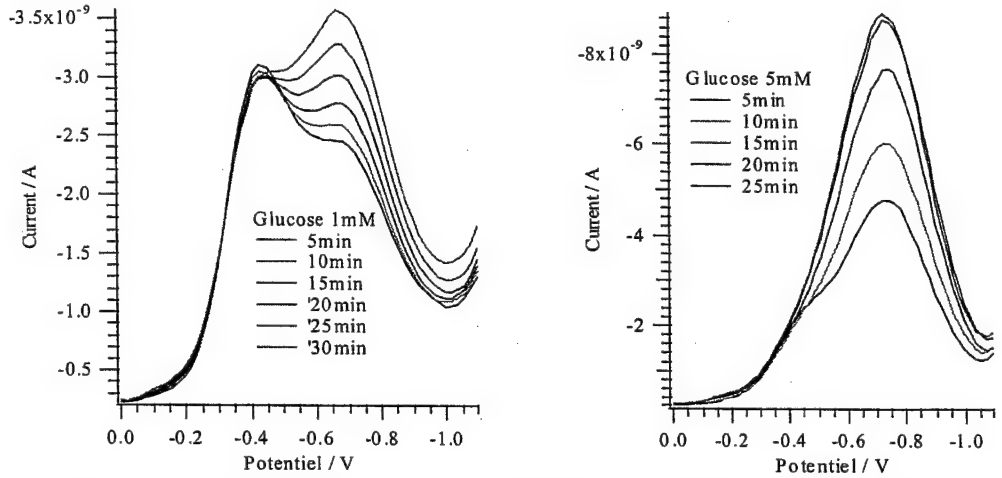

Figure 5: Time dependence on H_2O_2 formation for glucose 1mM and 5mM

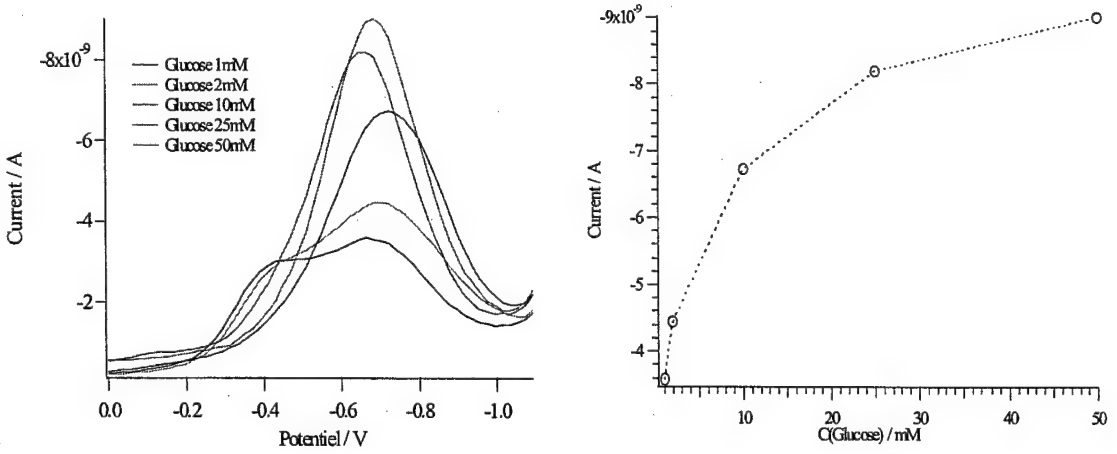

Figure 6: Calibration curve of glucose from 1 to 50mM.
The maximal Ipeak current was taken into account.

The reaction of glucose with GOx is slower at low concentration, and this is why the evolution of H_2O_2 is followed as a function of time.

For detection of lower glucose concentrations, GOx was adsorbed as previously described.
Solutions from 10µM to 200µM in PBS 10mM were used.
The parameters for DPV remained the same as those used in the previous experiments.

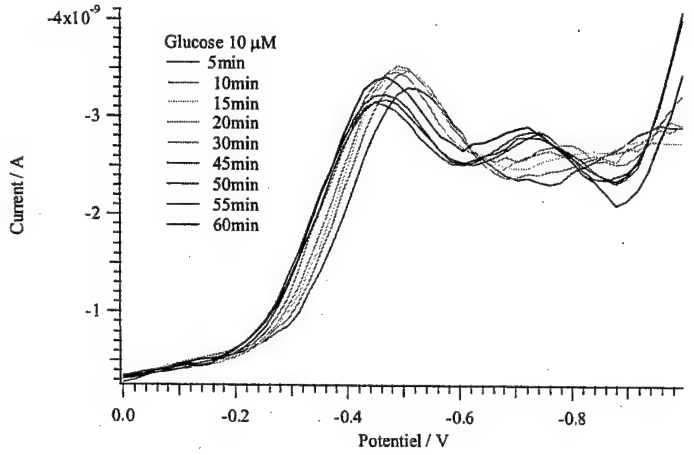

Figure 7: Detection of H_2O_2 vs time for a glucose 10µM in PBS 10mM

4.2.2. Coating of channel with GOx by reaction with anti-GOx

The channel was filled with a solution of 10mg/ml anti-GOx in PBS10mM. Having been eft at room temperature for about 30 minutes, a few microliters were pumped through the channel with a vacuum every 5 min to renew the anti-GOx.
The system was then washed with 50µl Tween 0.5% in PBS 10mM.
Non-specific adsorption was blocked with a solution of 0.2% BSA in PBS10mM. Washing was again performed and the device stored dry at 4°C.
Then, the channel was filled with a solution of 2200U/ml GOx in PBS 10mM and the reaction was allowed to proceed at room temperature during 1 hour before rinsing with PBS 10mM.
DPV measurements were then conducted as already described.

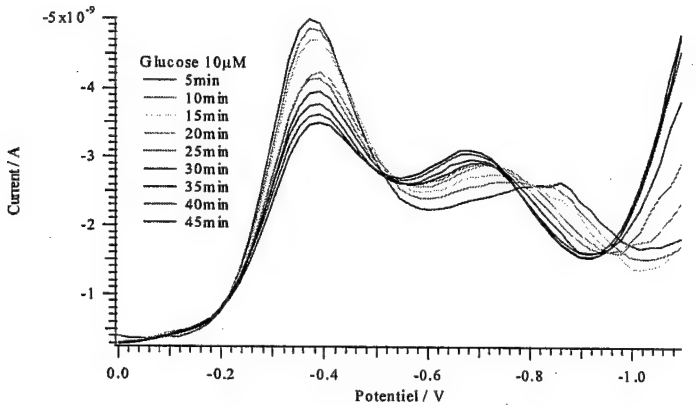

Figure 8: Evolution of H_2O_2 response for a solution of 10µM glucose in 10mM PBS.

A better response was observed for low glucose concentrations when GOx was immobilized by reaction with anti-GOx. Nevertheless, as shown in Figure 9, a quite different response for glucose 20µM was observed. No increase in the H_2O_2 peak was observed.

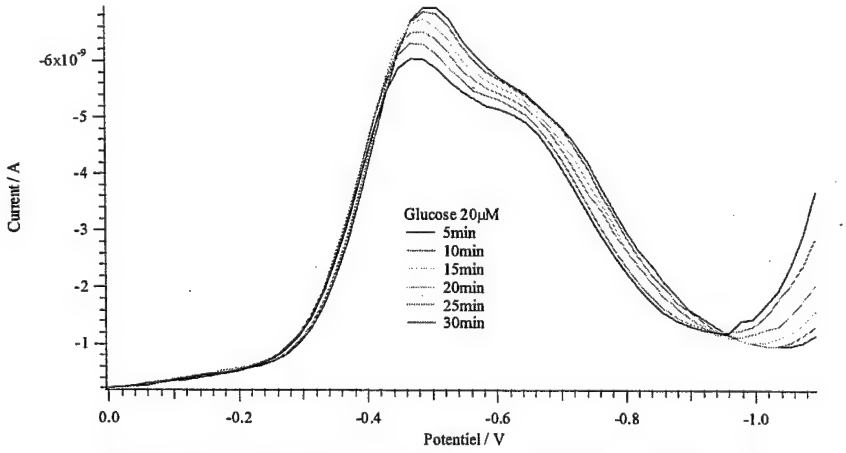

Figure 9: evolution of H_2O_2 vs. time for glucose 20µM

5. Conclusions

In the previous report, it was clearly demonstrated that the detection of glucose was possible on a gold electrode with and without mediator. Here, detection of lower glucose concentrations (in the micromolar range) is demonstrated. While optimisation of antibody adsorption is necessary, the sensitivity to H_2O_2 appears to have been increased by this technique of GOx immobilisation. A logical next step is to treat the channel, or more specifically the gold electrodes, so as to favorise the adsorption and to obtain a better detector response.

Addendum

Preliminary tests were also performed using lactate oxidase for detection of lactic acid. Solution from 0.5 to 4mM lactic acid were prepared by dilution in PBS 10mM. The lactate oxidase solution was 52U/ml in NaCl 140mM, pH=7.0. The setup and analysis conditions were the same as those for glucose detection.

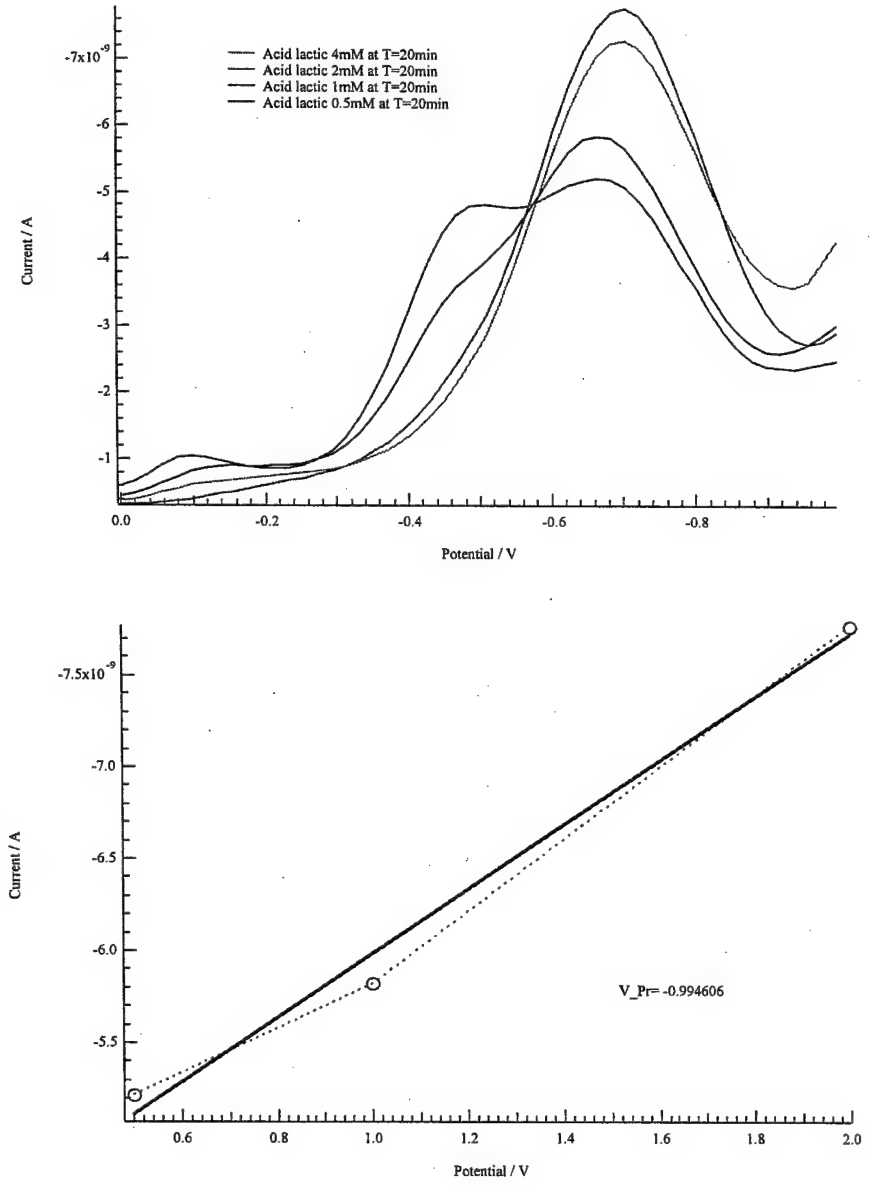

Figure 1: DPV of lactic acid from 0.5 to 4mM after 20 min reaction in the micro channel (upper panel), and calibration curve from 0.5mM to 2mM (lower panel)

Lactic acid quantification via H_2O_2 detection was demonstrated. The principle is identical to that for glucose. Further work on sensitivity is clearly envisaged.

NONINVASIVE MONITORING OF LACTATE

Preliminary results *in vitro* and *in vivo*

School of Pharmacy, University of Geneva

<u>*In vitro* extraction of L-lactate through pig ear skin</u>

Initial experiments investigating the reverse iontophoretic extraction of lactate were performed *in vitro* using excised porcine skin. The experimental set-up used is schematically illustrated below.

- Model: porcine skin
- Vertical diffusion cells
- Ag/AgCl electrodes
- 0.4 mA for 5 to 8 hours

<u>Donor compartment</u>:
L-Lactate 0,5 mM - 4,0 mM +
Hepes buffer 25 mM pH 7.4 +
NaCl 133 mM

<u>Electrode compartments</u>:
NaCl 0.5 mM

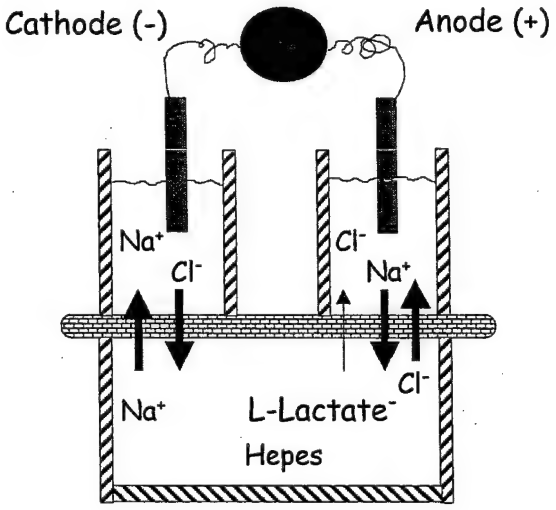

Lactate extracted to the anode was assayed every hour using an enzymatic method involving the liberation of NADH, which was detected fluorometrically.

The results are summarized in Figures 1(a-f). A reservoir of lactate in the skin is apparent (Figure 1a), a fact not surprising given that these experiments were performed on tissue that had been excised from recently sacrificed animals. When the extraction data from subdermal solutions containing fixed lactate concentrations (0.5 – 4 mM) are corrected for this 'reservoir', the reverse iontophoretic fluxes attain steady-state rates by 3 hours of iontophoresis (Figure 2), which depend linearly upon the subdermal analyte levels (Table 1 and Figure 3). It is seen that a period of more than one hour is necessary before the extraction becomes 'stable' and the slope of the flux versus concentration plot becomes essentially constant, with a satisfactory correlation coefficient. From 3 hours, the regressions are not significantly distinguishable.

***In vivo* extraction of Lactate across human skin**

Having shown that the reverse iontophoretic extraction of lactate was feasible in the *in vitro* model, a preliminary investigation in human volunteers was performed.

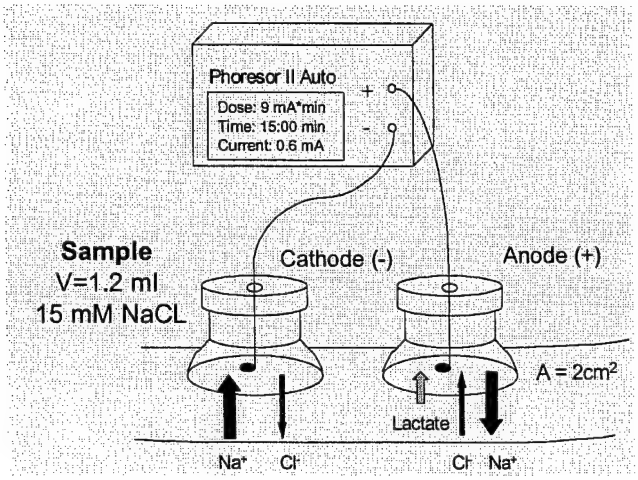

- *4 healthy volunteers*
- *15 min sampling intervals*
- *6 hours experiment*
- *0.3 mA/cm²*

1. *Analysis of lactate and chloride by High - Performance Ion Chromatography*
2. *Blood lactate measurements from finger-tip after each sampling interval*

The experimental design is illustrated above. Typically, two hours of iontophoresis was conducted to 'empty' the lactate reservoir from the skin before carrying out the 15-minute sampling protocol, with concomitant measurements of blood lactate via finger-lancing and measurement of the blood concentration with a commercially available device (Accusport, Roche Diagnostics, Switzerland). Extracted lactate and chloride, which acted as the internal standard, were determined chromatographically.

Table 2 presents the chloride extraction results and demonstrates that this ion is stably and efficiently transported across the skin by iontophoresis, as anticipated given its presence at high and fixed concentration subdermally, and its high mobility as a small, univalent anion. The calculated transport number of chloride from these data (i.e., the fraction of current flowing across the skin which is carried by this ion) is on the order of 0.4, a value quite consistent with that reported in the literature.

Figure 4 shows the individual results from each of the five experiments performed. Two graphs are presented for each individual run. On the left, the iontophoretically extracted lactate fluxes (in blue) are compared to the intermittent measurements of blood lactate levels (in red). Although there are significant periods of good correlation between these parameters, there are also moments where this consistency is lost. This is more easily seen in the graphs on the right of the page which plot the ratio of extracted lactate flux to the corresponding blood level as a function of time. This ratio (K) has units of μL/hr and is defined as follows:

$$K = J_{lactate}/[lactate]_{blood}$$

Visual inspection of these K values suggests that they separate into two groups (Table 3). The most significant category is the stable subset, with an average value (K_1) of around 60 μL/hr. The second group (which has been divided, somewhat arbitrarily into two) manifests K values which are significantly higher. Often, these elevated numbers are perceived towards the end of the experimental runs, leading one to an interesting hypothesis about the possibility of local effects on lactate extraction – recall that the subjects' arms at this point had remained essentially immobilized for 5 or 6 hours. The last panel in Figure 4 attempts to capture this information in a single depiction of all K values plotted as a function of time. While the overall reasonable agreement and consistency between subjects is apparent, the deviations stand out quite obviously.

Self-evidently, there is additional work to be done here. Nevertheless, the initial findings are, on the whole, quite encouraging and fully support further concentrated effort on the reverse iontophoretic extraction and monitoring of this important metabolite.

Figures 1.a-f

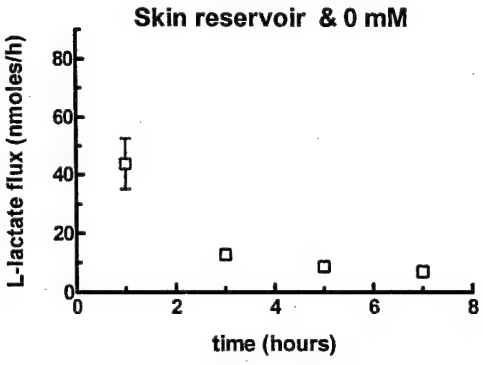
Skin reservoir & 0 mM
L-lactate flux (nmoles/h)
time (hours)

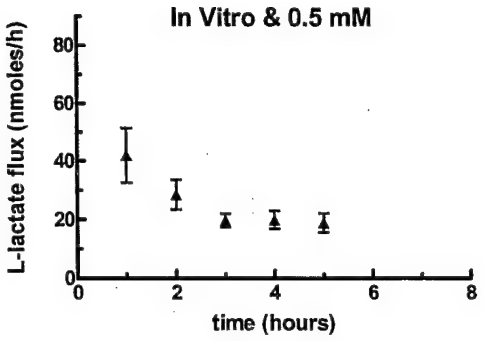
In Vitro & 0.5 mM
L-lactate flux (nmoles/h)
time (hours)

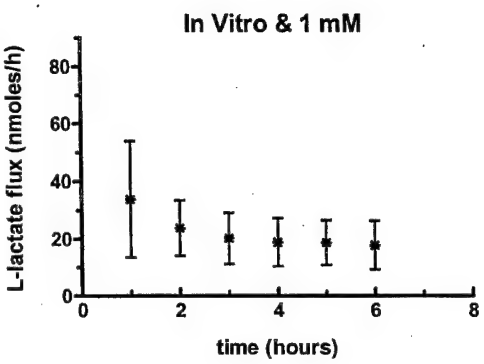
In Vitro & 1 mM
L-lactate flux (nmoles/h)
time (hours)

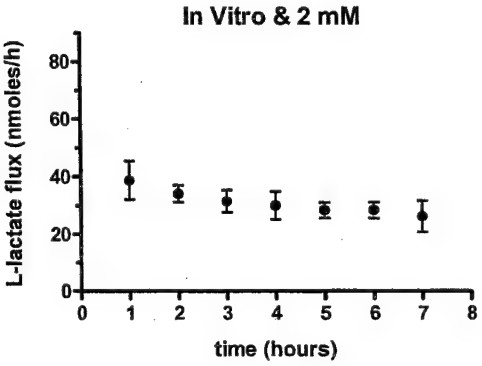
In Vitro & 2 mM
L-lactate flux (nmoles/h)
time (hours)

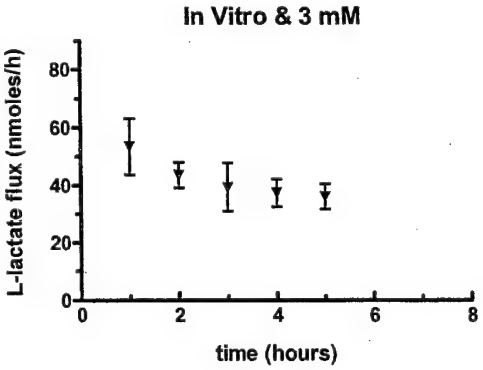
In Vitro & 3 mM
L-lactate flux (nmoles/h)
time (hours)

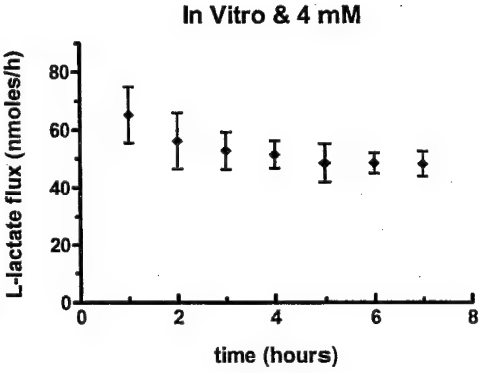
In Vitro & 4 mM
L-lactate flux (nmoles/h)
time (hours)

Figure 2

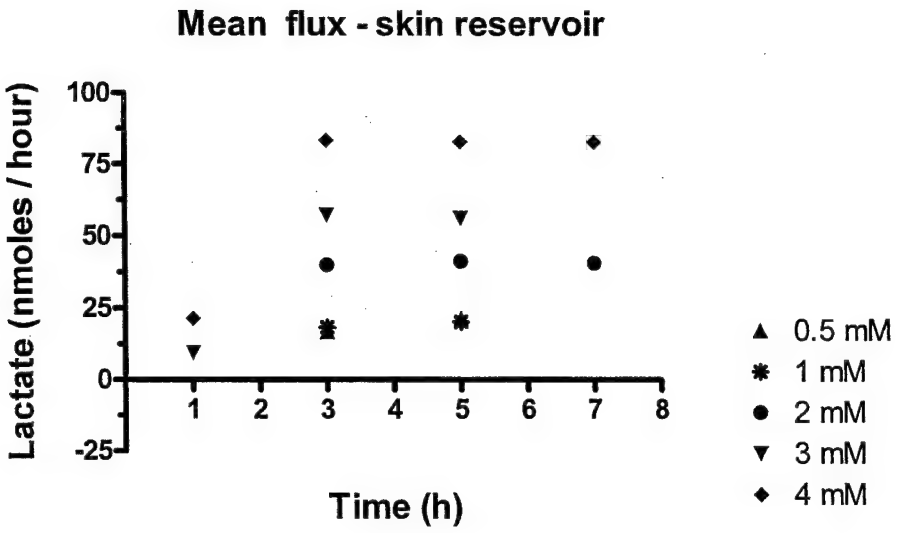

Figure 2: Lactate reservoir effect. The figure shows the average L-lactate fluxes measured at 1, 3, 5 and 7 hours for the different subdermal concentrations tested and after subtraction of the average reservoir fluxes measured in the experiment performed without L-lactate.

Table 1: Regressions of the data shown in Figures 3.a-f according to the equation "Flux" = k • "Concentration" + Intercept, where "Flux" corresponds to the anodal extraction flux of lactate in nanomoles/hour and "Concentration" is the subdermal level of the drug in mM.

Time (hr)	k [a]	Intercept [b]	r^2
1	7.22 ± 1.73	31.44 ± 3.91	0.3395
2	8.86 ± 1.07	18.26 ± 2.53	0.6890
3*	9.40 ± 0.85	13.12 ± 1.93	0.7815
4*	9.41 ± 0.83	11.56 ± 1.98	0.8034
5*	9.03 ± 0.70	10.80 ± 1.56	0.8343

[a] Units are (μL/hour);

[b] Units are (nanomoles/h)

* Pooled k and intercept values are 9.27 μl/h and 11.84 nanomoles/h.

Figures 3.a-f

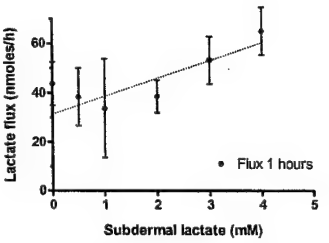

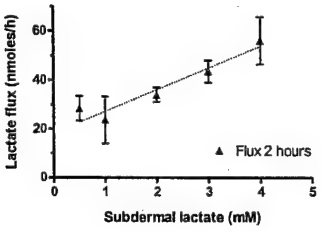

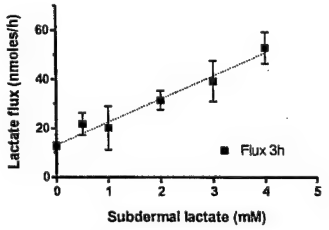

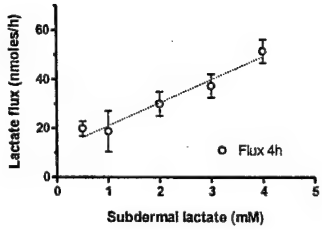

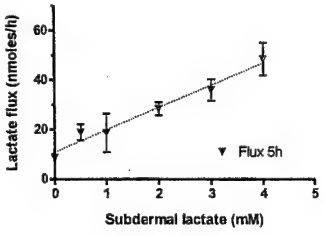

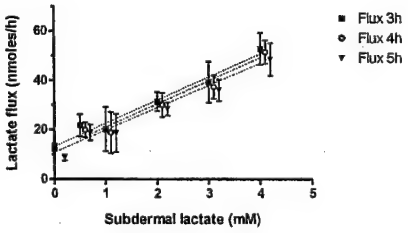

Table 2: Chloride anodal extraction fluxes (μmoles/hour) measured for each volunteer and experiment.

	S.1-Expt.2	S.1-Expt.3	S.2-Expt.1	S.3-Expt.1	S.4-Expt.1
Mean	9.93	12.64	9.55	9.10	8.02
S.D.	0.57	1.50	0.70	0.95	1.17
C.V. (%)	5.77	11.85	7.32	10.39	14.60
n*	15	14	18	16	16

- Total n was 20. Missing values were aberrant (Dixon test , p=0.95).

Table 3: Values of K (μL/hour), i.e., $J_{lactate}/[lactate]_{blood}$ for each subject and experiment. Values are expressed as mean ± S.D.

	S.1-Expt.2	S.1-Expt.3	S.2-Expt.1	S.3-Expt.1	S.4-Expt.1
K_1	51.3 ± 10.7	55.6 ± 9.5	59.6 ± 13.0	72.7 ± 6.3	58.2 ± 3.4
n	12	7	11	11	4
K_{2a}		129.9 ± 4.7	214.8		158.8 ± 37.9
n		4	1		7
K_{2b}		281.2			221.2
n		1			1

Figures 4.a-f

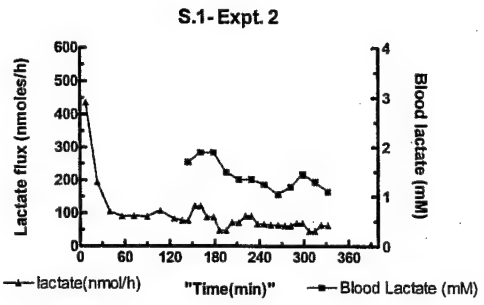
S.1- Expt. 2
Lactate flux (nmoles/h)
Blood lactate (mM)
lactate(nmol/h)
"Time(min)"
Blood Lactate (mM)

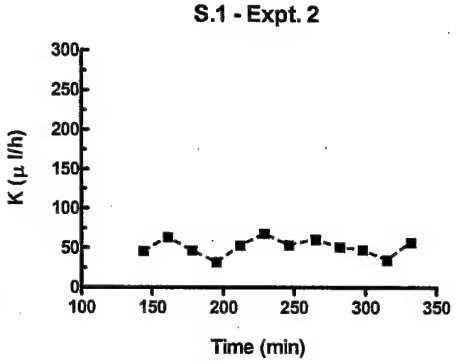
S.1 - Expt. 2
K (μ l/h)
Time (min)

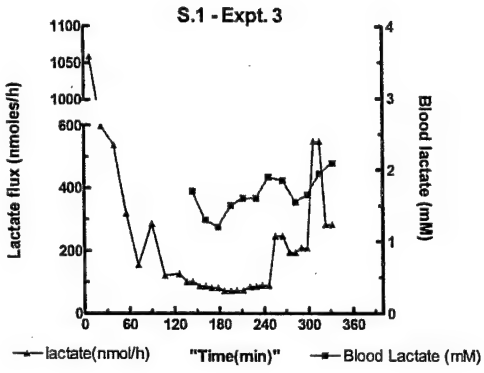
S.1 - Expt. 3
Lactate flux (nmoles/h)
Blood lactate (mM)
lactate(nmol/h)
"Time(min)"
Blood Lactate (mM)

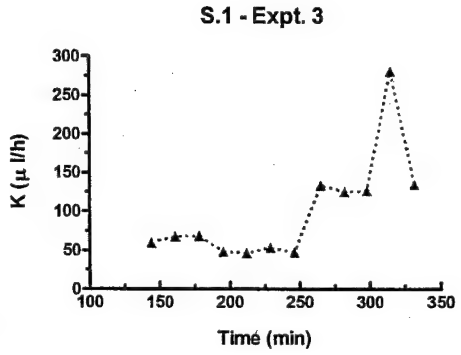
S.1 - Expt. 3
K (μ l/h)
Time (min)

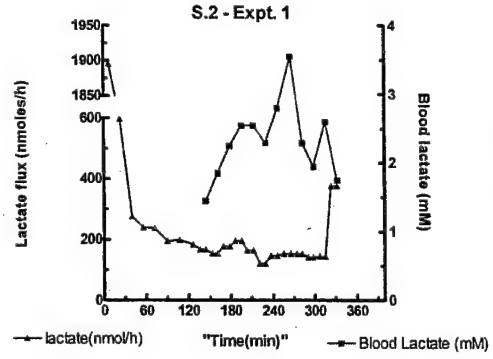
S.2 - Expt. 1
Lactate flux (nmoles/h)
Blood lactate (mM)
lactate(nmol/h)
"Time(min)"
Blood Lactate (mM)

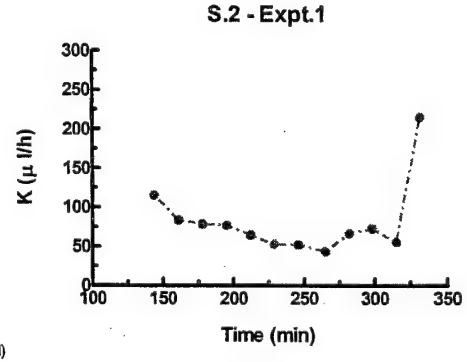
S.2 - Expt.1
K (μ l/h)
Time (min)

Figures 4.g-k

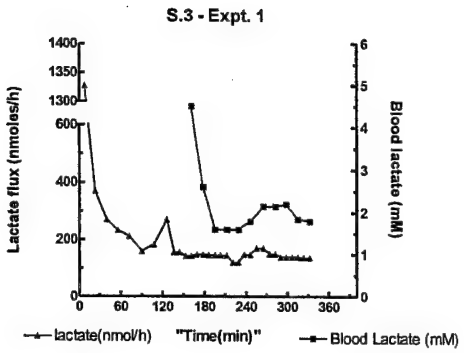
S.3 - Expt. 1
Lactate flux (nmoles/h)
Blood lactate (mM)
lactate(nmol/h)
"Time(min)"
Blood Lactate (mM)

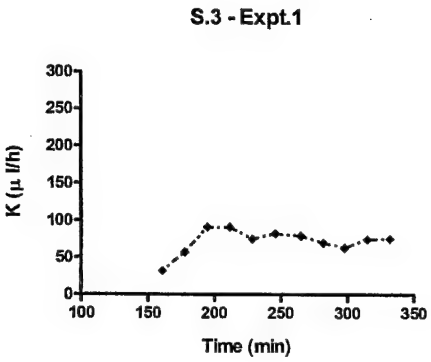
S.3 - Expt.1
K (μ l/h)
Time (min)

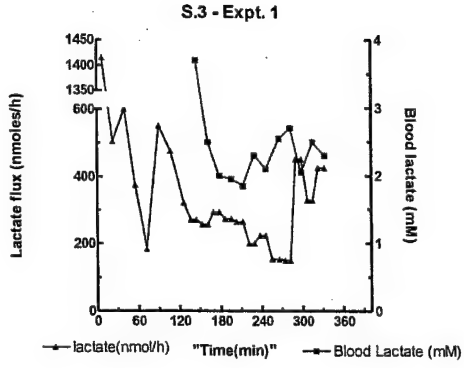
S.3 - Expt. 1
Lactate flux (nmoles/h)
Blood lactate (mM)
lactate(nmol/h)
"Time(min)"
Blood Lactate (mM)

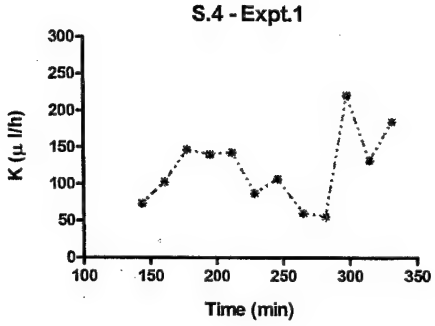
S.4 - Expt.1
K (μ l/h)
Time (min)

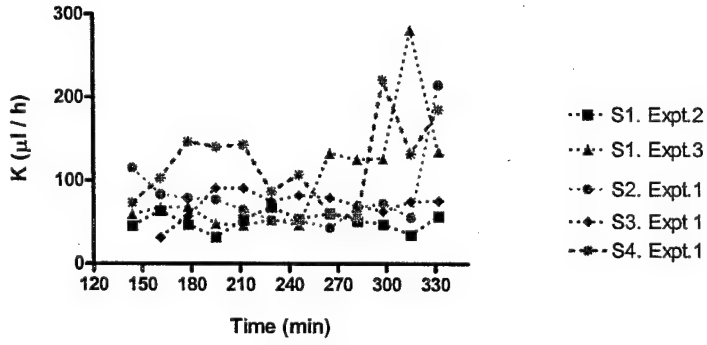
K (μl / h)
Time (min)
S1. Expt.2
S1. Expt.3
S2. Expt.1
S3. Expt 1
S4. Expt.1

Key accomplishments

1. The GlucoWatch Biographer uses reverse iontophoresis to extract glucose across the skin to monitor glycemia in diabetes. The invasive daily calibration with a conventional "fingerstick" has been perceived as disadvantage. Here, an "internal standard" is used so as to render the approach completely non-invasive. The simultaneous extraction of glucose and sodium by reverse iontophoresis was performed on human volunteers over 5 hours, and blood glucose was measured in the conventional manner at each collection interval. These data were used for each subject to calculate an extraction constant (K), which equals the ratio of the extracted fluxes (J_{glc}/J_{Na+}) normalized by the corresponding ratio of the concentrations in the blood ([glu]/[Na^+]). The values of K were compared between and within subjects. The iontophoretically extracted glucose flux reflected the glucose concentration profiles in the blood, sodium extraction remained essentially constant consistent with the fact that its systemic concentration does not vary significantly. A constant value of K was established for part of the study population, therefore, allowing for an accurate prediction of glycemia without the need for a calibrating blood sample. However, further experimentation in additional subjects revealed seasonal changes in the efficiency of glucose extraction, that were not mirrored by the reverse iontophoresis of Na^+. That is, variation in K became apparent. The "internal standard" should be useful for the determination of glycemia by reverse iontophoresis without calibrating with a blood sample. While Na^+ can be a useful internal standard, this research demonstrates that a neutral molecule, extracted by the same mechanism as glucose, would represent a better alternative. {Paper to be submitted to *Clinical Chemistry*}

2. The development of a method to detect glucose electrochemically, without a mediator, in a polymeric microchip. The method appears, furthermore, to be easily adaptable to lactate monitoring.

3. A preliminary proof-of-concept demonstration that reverse iontophoresis can be applied to the noninvasive monitoring of lactate. Experiments in a model system using excised porcine skin established the linearity of lactate extraction. Subsequently, initial studies in human volunteers have revealed that the approach is feasible.

4. Three alkali cations, potassium, sodium and lithium, have been separated within 15 seconds in a 1 cm long polymer microchip. The separation microchannel is modified by a poly-cation, poly(allylammonium chloride), which makes the channel surfaces positively charged leading to a reversed electroosmotic flow (EOF) when compared to bare channels. Due to the decreased apparent mobility of the cations, the separation resolution is improved allowing the use of shorter channels. {Ms in preparation – see appendix}

Reportable outcomes

One paper has been published already:

Reverse iontophoresis for noninvasive glucose monitoring: The internal standard concept. A. Sieg, R.H. Guy and M.B. Delgado-Charro. *J. Pharm. Sci.*, **92**: 2295-2302 (2003).

Two additional manuscripts should be submitted shortly:

Polyelectrolyte modified short microchannel for cation separation. X. Bai, C. Roussel, H. Jensen and H.H. Girault.

Non-invasive glucose monitoring by reverse iontophoresis *in vivo*: Application of the internal standard concept. A. Sieg, R.H. Guy and M.B. Delgado-Charro. *Clin. Chem.*

An extended abstract has also been published:

Calibration-free glucose monitoring using reverse iontophoresis *in vivo*. A. Sieg, R.H. Guy and M.B. Delgado-Charro. *Proc. Int. Symp. Control. Rel, Bioact. Mater.* **30**: # 126 (2003).

Conclusions

In less than 9 months, the project has made considerable progress in both glucose and lactate monitoring by reverse iontophoresis. Glucose is further advanced, with significant *in vivo* data built upon the *in vitro* findings. Novel, micro-chip detection and analysis devices are in development with considerable promise of miniaturization and high sensitivity and precision.

A one-year, no-cost extension has been granted which should allow further, additional progress towards the project's goals, and an opportunity to capitalize upon the promising lactate results presented here.

Appendix

Polyelectrolyte modified short microchannel for cation separation. X. Bai, C. Roussel, H. Jensen and H.H. Girault. *Manuscript in preparation.*

Polyelectrolyte modified short microchannel for cation separation

Xiaoxia Bai, Christophe Roussel, Henrik Jensen and Hubert H. Girault*

Laboratoire d'Electrochimie Physique et Analytique, Institut de Chimie Moléculaire et Biologique, Ecole Polytechnique Fédérale de Lausanne, 1015 LAUSANNE, Switzerland; Tel.: +41.21.693.31.51; Fax: +41.21.693.36.67; E-mail: hubert.girault@epfl.ch

Abbreviations

Micro total analysis systems: μTAS
Electroosmotic flow: EOF
Capillary electrophoresis: CE
Polyethylene terephthalate: PET
Polyethylene: PE
2-(N-morpholino(ethanesulfonic acid): MES
L-histidine: His
Poly(allylamine hydrochloride): PAA-HCl
Hydroquinone: HQ
Background electrolyte: BGE

Keywords: Capillary electrophoresis, cation separation, polyelectrolyte, surface modification, microchannel

Abstract

Three alkali cations, potassium, sodium and lithium, have been separated within 15 seconds in a 1 cm long polymer microchip. The separation microchannel is modified by a poly-cation, poly(allylammonium chloride), which makes the channel surfaces positively charged leading to a reversed electroosmotic flow (EOF) when compared to bare channels. Due to the decreased apparent mobility of the cations, the separation resolution is improved allowing the use of shorter channels.

1. Introduction

Micro total analysis systems (μTAS) allow fast and efficient chemical separation within small volumes. This is the main reason why they have attracted so much interest in the recent years[1]. For pumping, electro-osmotic flow (EOF) is usually the method of choice as it is rather easy to implement experimentally compared to pressure driven flow[2-5]. However, the main weakness of EOF is the stability of the flow rate, and perhaps this is why capillary electrophoresis (CE) as a separation technique is not always as reproducible as required. To stabilize the EOF, it has been proposed to control the pH of the eluent, or to fix the zeta potential of the capillary either by chemical modification or by adsorption. In the latter case, adsorption of polyelectrolytes is rather an easy route to achieve this goal[6-10]. Except for modulating the EOF, these adsorption methods, both covalent and non-covalent, have also been used to prevent non-specific adsorption, or as a means to attach active molecules (such as antibodies) to the surface. In the present paper, we demonstrate that polyelectrolyte adsorption can be used both to obtain a stable EOF as well as to improve the separation efficiency.

The separation of small ions is routinely carried out by traditional CE in silica capillaries[11-19], the ions being typically separated in minutes when the capillary length ranges from 10 to 80 centimetres. Analysis of small inorganic/ organic charged species has also been performed on microchip platforms by capillary zone electrophoresis. For example, separation of potassium, lithium and sodium[20] was observed on a 8.4 cm long glass microchip within a minute. Calcium and magnesium have also been separated within 15 seconds in a 2.5 cm long quartz microchip[21]. The separation of ammonium, methylammonium and sodium has been obtained within 40 seconds in a 4 cm long polymer chip by using a movable contactless-conductivity detector[22].

Fast anion separation has been obtained using the co-electroosmotic separation mode on adding a cationic surfactant to the electrolyte that reverses the EOF, so that the anionic solutes electrophoretically migrate in the same direction as EOF[23-25]. Here the same methodology is applied to generate a counter-electroosmotic mode of cation separation in order to decrease the length of the capillary. The length, as one of the size parameters, is an important aspect of microchip design where patterning density is a major issue. The present work describes a capillary electrophoresis analysis of Li^+, Na^+ and K^+ on a polymer chip using a polyelectrolyte coating of the micro-channel surface with the objectives of performing a separation in 15 seconds within a 1 cm long separation channel. The long-term objective of this work is to design a lithium sensor for EOF reversed electrophoresis of extracted sub cutaneous fluid where sample volume is a major issue.

2. Materials and methods

2.1 Chemicals

Polyethylene terephthalate (PET) sheets (100 μm thick Melinex) were purchased from Dupont (Geneva, Switzerland). 2-(N-morpholino (ethanesulfonic acid (MES), L-histidine (His), poly(allylamine hydrochloride) (PAA-HCl) and hydroquinone (HQ) were obtained from Sigma (St. Louis, MO, USA). The standard ionic solutions with a concentration of

0.1 M were from Fluka (Buchs, Switzerland). Milli-Q water (Millipore, Bedford, MA, USA) was used to prepare all solutions. Freshly prepared solutions were used for the experiments.

2.2 Microchip fabrication

The fabrication of microchip has been previously described[26]. Briefly, the PET sheet is photoablated by a UV excimer laser (Argon Fluor Excimer Laser at 193 nm, Lambda Physik LPX 2051, Göttingen, Germany). The typical channel obtained has a trapezoidal cross-section shape. Carbon ink is pasted into a photoablated micro channel (with a depth of 20 μm and a width of 100 μm) and dried at 80 °C for 30 minutes to form a conductive track. A photo resist solution (Shipley Europe limited, Herald Way, Coventry, CV3 2RQ, UK) is used to seal and protect the carbon track, by spin-coating over the carbon track and thermally treating at 90 °C for 1 hour. In a second step, the main separation channel (corresponding to the horizontal channel shown in figure 1a) is photoablated perpendicularly to the carbon track so as to expose two face-to-face microelectrodes on the opposite vertical walls of the separation channel as shown in figure 1b. The separation channel is usually about 40 μm deep, 50 μm wide at the top. Two side channels (corresponding to the two vertical side channels shown in figure 1a) are photoablated for injection purposes, which feature a so-called double-T design with a typical center-to-center distance of 100 μm, the microchip obtained is thermally laminated by a polyethylene/polyethylene terephthalate (PE/PET) layer (35 μm thick, Morane, Oxon, UK) at 135 °C and 2 bars. The obtained microchip is similar to that shown in figure 1a (the top view) and figure 1b (the cross-section) except the effective separation length (from the double-T to the detection electrode) which may be different depending on the chip surface chemistry. The chip shown in figure 1a is indeed a polycation coated microchip that has a shorter effective length of 1 cm.

2.3 CE on microchip

The microelectrodes are connected to a Metrohm conductivity meter (732 conductivity detector, Metrohm, Switzerland) controlled by a PC through an interface (762 interface, Metrohm)[27]. A floating battery with 5 kV output and a locally made switching box are controlled by a PC through a Labview VI program (National Instrument, Austin, TX 78759-3504, USA). An electrokinetic floating injection is used to inject the sample: a positive potential of 500 V is applied for 20s between the sample and sample waste reservoirs to fill the sample segment of the channel between these two reservoirs while the buffer and waste reservoirs are kept floating (no pinch). A positive potential of 800 V or 2 kV is applied between the buffer reservoir and the waste reservoir during a typical separation time of 50s whilst the sample reservoirs are floating. Special attention has been given to the volume of the solutions in all the reservoirs. It is observed that when the solution volume in the buffer reservoir is smaller than that of other reservoirs, the sample plug in the double T section migrates to the buffer reservoir during injection due to the effect of the hydrodynamic pressure, and a sample leakage from the sample channel to the main channel is observed after injection.

A solution of 20 mM MES with 20 mM His (pH at 6) is used as background electrolyte (BGE) to separate cations[18]. Hydroquinone is added in the BGE to avoid the bubble generation due to an electrical cross-talk between the AC detection field (between the

two face-to-face carbon electrodes) and the main DC high voltage. According to the redox potential of hydroquinone (0.699 V vs. SHE), it can be easily oxidised into benzoquinone before water (1.23 vs. SHE) to prevent the electrolysis of water that leads the formation of hydrogen (at cathode) and oxygen (at anode).
The EOF measurement follows Huang's current monitoring method[28]. The principle of the measurement is to follow the conductivity change in a channel by monitoring the current at a constant voltage. When a solution of slightly higher conductivity is pumped (using a high voltage) inside a micro-channel containing the same solution with lower conductivity, an increase and finally a stabilization of the current is observed, which indicates the time required by the solution to run through the channel. Measurement is performed with 4 mM and 20 mM MES/His solutions to obtain an obvious current change, and a typical electrical field of 330 V/cm (by Spellman CZE 1000R Power Supply, Hauppauge, NY, USA) is applied to the micro-channel.

2.4 Surface modification of microchannel

The surface modification of PET channel by PAA-HCl is similar to that previously published work[29]. It was reported that the PAA-HCl absorbs on PET at low pH but reacts by amidation at high pH as a free base to form a covalently attached PAA-HCl layer. Therefore, PET-NH_2 samples prepared at high pH (such as 11.5) contain physisorbed PAA-HCl as well as chemisorbed PAA-HCl.
Briefly, after washing with distilled water, the microchannel is filled with a PAA-HCl solution of 0.02 M repeat unit (corresponding to the concentration of the monomer) at pH 11.5 (adjusted by addition of 0.1 M NaOH) for 1 hour. The channel is washed again with distilled water before filling with HCl (pH=2) for 30 minutes. The channel finally needs to be cleaned by distilled water and kept in air when it is not in use. The formation of the PAA-HCl layer is confirmed by EOF measurements. The electro-osmotic mobility of a bare PET channel was measured to be $3.15 \cdot 10^{-4}$ $cm^2V^{-1}s^{-1}$ and the electro-osmotic mobility of a PAA-HCl coated PET channel was $-3.52 \cdot 10^{-4}$ $cm^2V^{-1}s^{-1}$. It shows that the magnitude of the electro-osmotic mobility does not change much after surface coating, but the flow direction is reversed. This layer is quite stable when the chip is kept in air, similar results can be reproduced after several days.

3. Result and discussion

A baseline separation of three cations, potassium, sodium and lithium, is obtained in a bare PET microchip with an effective length of 4.5 cm (electric field of 308V/cm), as shown in figure 2. The resolutions between potassium and sodium, sodium and lithium are 2.14 and 1.63, respectively. The theoretical plate number is calculated as 35600/m for potassium ion.
The resolution of the separation is given by

$$R_s = \frac{t_2 - t_1}{\frac{1}{2}(w_1 + w_2)} \qquad (1)$$

where t is the migration time and w is the baseline bandwidth of the signal, is proportional to the difference of the migration time, Δt. This difference can be expressed in terms of the apparent mobility u

$$\Delta t = t_2 - t_1 = \frac{L}{E}\left(\frac{u_2 - u_1}{u_1 u_2}\right) \quad (2)$$

where L is the effective length of the separation channel, E is the electrical field strength. The resolution is also related to the width of the peak, which can be represented by the variance σ and therefore to the apparent mobility,

$$w = 4\sigma = 4\sqrt{2Dt} = 4\sqrt{\frac{2DL}{E}\cdot\frac{1}{u}} \quad (3)$$

where D is the diffusion coefficient. Then, the separation resolution can be written as

$$R_s = \frac{u_2 - u_1}{u_2\sqrt{u_1} + u_1\sqrt{u_2}}\sqrt{\frac{L}{8DE}} \quad (4)$$

The apparent mobility is the sum of the electro-osmotic mobility and the electrophoretic mobility. The sign of the former depends on the sign of the zeta potential. For a bare channel, the charges on the channel are negative, e.g. carboxy groups, the zeta potential is therefore negative and the electro-osmotic mobility is positive, i.e. the EOF goes in the same direction as the electric field. The sign of the electrophoretic mobility depends on the sign of the ions, and is positive for the cations. By reversing the charges on the microchannel walls by adsorption of the polycation, the electro-osmotic mobility becomes negative. The difference u_2–u_1 in Eqn. (2) is not altered by reversing the flow direction, but the apparent mobility u of the cations becomes smaller when the flow is reversed. Indeed, for a bare channel the electro-osmotic and the electrophoretic mobilities add for cations, whereas in the modified channel the electro-osmotic mobility is subtracted from the electrophoretic one. As a consequence, the ratio $\frac{1}{u_2\sqrt{u_1} + u_1\sqrt{u_2}}$ is increased upon the modification of the channel. In other words, to obtain a similar separation with a fixed resolution, either the length of the channel could be decreased or the electrical field strength could be increased.

The following experiment confirms this approach. A microchip with a short effective separation length, 1 cm (as shown in figure 1a), is used to separate the same cations as mentioned before. The electrophoregrams obtained in this microchip before and after PAA-HCl coating are compared in figure 3. As it can be seen from figure 3a, although each ion has not been identified respectively, the three ions cannot be separated in the bare PET microchannel when the electrical field is 296 V/cm., i.e. about the same electric field strength as in figure 2. It has to be pointed out that, the other broadening effects such as the detector region width and the injection plug width may improve the detected signal. For instance, the separation can be accelerated by injecting a very small plug, and a confocal fluorescence detection focusing in the center of the channel can also improve the resolution of the separation[30]. However, those are out of the scope of the present work and therefore have not been evaluated here. According to Eqn. (4), when the effective separation length is decreased by a certain factor, the electrical field should be decreased by the same factor in order to obtain a separation with the same resolution. For this microchannel with an effective length of 1 cm, the electrical field should be 68 V/cm to

obtain a separation similar to that shown in figure 2. When the channel is coated with a PAA-HCl layer, a baseline separation is obtained even at an electrical field of 740.7 V/cm, as shown in figure 4b. With this flow reversal method, a high electrical field, instead of a much lower electrical field as in the usual CE, can be applied when the effective length is highly decreased. The resolution between potassium and sodium is calculated to be 1.68 and 1.23 between sodium and lithium. The relatively small value of the resolution between sodium and lithium is mainly due to the broadening of the lithium signal. The theoretical plate number for potassium is 29000/m. Compared to the separation shown in figure 2, both the resolution and the theoretical plate number are only slightly decreased. As shown in Eqn. (2) & (4), the migration time can be further decreased by increasing the applied electrical field, at the cost of reduced resolution (linear dependence *vs* square root dependence). Those data show that the short channel coated with a PAA-HCl layer yields a similar electrophoresis efficiency for the small cations separation compared to the longer bare channel.
The presented experiments show a separation of cations for whose electrophoretic mobility is higher than the electro-osmotic one. This method can also be applied to cations that have relatively small electrophoretic mobility. In this case, the electric field direction needs to be reversed for the cations to pass the detector and the apparent mobility is then negative.

Conclusion

The presented work develops a surface modification method for polymer microchip to decrease the effective separation length of the chip whilst maintaining the resolution. This is important to micro device design strategies as micro-fabrication techniques impose restriction on the size of the devices. The present method therefore allows higher packing densities when fabricating CE e.g. by plasma etching methods[31].

Acknowledgement

The authors wish to thank Metrohm (CH) and the Swiss Commission for Technology and Innovation (CTI: 4421.2) and Professor R. Guy (University of Geneva) and the US army medical research (DAMD17-02-1-0712) for financial support.

References

(1) Reyes, D. R.; Iossifidis, D.; Auroux, P. A.; Manz, A. *Analytical Chemistry* **2002**, *74*, 2623-2636.
(2) Dolnik, V.; Liu, S. R.; Jovanovich, S. *Electrophoresis* **2000**, *21*, 41-54.
(3) Bousse, L.; Cohen, C.; Nikiforov, T.; Chow, A.; Kopf-Sill, A. R.; Dubrow, R.; Parce, J. W. *Annual Review of Biophysics and Biomolecular Structure* **2000**, *29*, 155-181.
(4) Bruin, G. J. M. *Electrophoresis* **2000**, *21*, 3931-3951.
(5) Lacher, N. A.; Garrison, K. E.; Martin, R. S.; Lunte, S. M. *Electrophoresis* **2001**, *22*, 2526-2536.
(6) Graul, T. W.; Schlenoff, J. B. *Analytical Chemistry* **1999**, *71*, 4007.
(7) Liu, Y.; Fanguy, J. C.; Bledsoe, J. M.; Henry, C. S. *Analytical Chemistry* **2000**, *72*, 5939-5944.
(8) Barker, S. L. R.; Tarlov, M. J.; Canavan, H.; Hickman, J. J.; Locascio, L. E. *Analytical Chemistry* **2000**, *72*, 4899-4903.
(9) Barker, S. L. R.; Ross, D.; Tarlov, M. J.; Gaitan, M.; Locascio, L. E. *Analytical Chemistry* **2000**, *72*, 5925-5929.
(10) Kamande, M. W.; Kapnissi, C. P.; Zhu, X. F.; Akbay, C.; Warner, I. M. *Electrophoresis* **2003**, *24*, 945-951.
(11) Gross, L.; Yeung, E. S. *Analytical Chemistry* **1990**, *62*, 427.
(12) Beck, W.; Engelhardt, H. *Chromatographia* **1992**, *33*, 313-316.
(13) Lin, T. I.; Lee, Y. H.; Chen, Y. C. *Journal of Chromatography A* **1993**, *654*, 167-176.
(14) Shi, Y.; Fritz, J. S. *Journal of Chromatography A* **1994**, *671*, 429.
(15) Mayrhofer, K.; Zemann, A. J.; Schnell, E.; Bonn, G. K. *Analytical Chemistry* **1999**, *71*, 3828-3833.
(16) Francois, C.; Morin, P.; Dreux, M. *Journal of Chromatography A* **1995**, *706*, 535-553.
(17) Soga, T.; Ueno, Y.; Naraoka, H.; Matsuda, K.; Tomita, M.; Nishioka, T. *Analytical Chemistry* **2002**, *74*, 6224.
(18) Kuban, P.; Kuban, P.; Kuban, V. *Electrophoresis* **2002**, *23*, 3725.
(19) Tanyanyiwa, J.; Hauser, P. C. *Electrophoresis* **2002**, *23*, 3781.
(20) Gardeniers, H.; Mulder, M.; Luttge, R.; van den Berg, A. *MST-News* **2002**, *4*, 39.
(21) Kutter, J. P.; Ramsey, R. S.; Jacobson, S. C.; Ramsey, J. M. *Journal of microcolumn separations* **1998**, *10*, 313.
(22) Wang, J.; Chen, G.; AMuck, A. J. *Analytical Chemistry* **2003**, *75*, 4475-4479.
(23) Zemann, A.; Nguyen, D. T.; Bonn, G. *Electrophoresis* **1997**, *18*, 1142-1147.
(24) Cugat, M. J.; Borrull, F.; Calull, M. *Chromatographia* **1999**, *50*, 229-234.
(25) Cugat, M. J.; Borrull, F.; Calull, M. *Chromatographia* **1999**, *49*, 261-267.
(26) Roberts, M. A.; Rossier, J. S.; Bercier, P.; Girault, H. H. *Analytical Chemistry* **1997**, *69*, 2035.
(27) Bai, X.; Lee, H. J.; Rossier, J. S.; Reymond, F.; Schafer, H.; M., W.; Girault, H. H. *Lab on a Chip* **2002**, *2*, 45.
(28) Huang, X. H.; Gordon, M. J.; Zare, R. N. *Analytical Chemistry* **1988**, *60*, 1837-1838.

(29) Chen, W.; McCarthy, T. J. *Macromolecules* **1997**, *30*, 78-86.
(30) Bai, X. X.; Josserand, J.; Jensen, H.; Rossier, J. S.; Girault, H. H. *Analytical Chemistry* **2002**, *74*, 6205-6215.
(31) Rossier, J. S.; Vollet, C.; Carnal, A.; Lagger, G.; Gobry, V.; Girault, H. H.; Michel, P.; Reymond, F. *Lab on a Chip* **2002**, *2*, 145-150.

Figure Legends

Figure 1: Scheme of the top view of microchip (a) and the cross-section at the detector position (b). Two 0.9 cm long side channels (vertical) feature a double-T for injection purpose, two face-to-face microelectrodes are perpendicularly located at the end of the main separation channel.

Figure 2: Electrophoregram of ions. Channel dimension is 50 μm wide, 40 μm deep and with 4.5 cm effective separation length; sample is 1 mM K^+, Li^+ and Na^+, that is injected at 500 V for 25 s and separated at an electrical field of 308 V/cm; BGE : 20 mM MES/His, pH at 6.

Figure 3: Comparison of the electrophoregrams obtained in microchip before (a) and after (b) a PAA-HCl coated layer on the channel surface. The effective length is 1 cm, the sample is injected at 500 V for 20 seconds and separated at an electrical field of 296 (a) or 741 V/cm (b), BGE: 20 mM MES/His+4 mM HQ, pH at 6. Other conditions are same as figure 2.

Figure 1

a

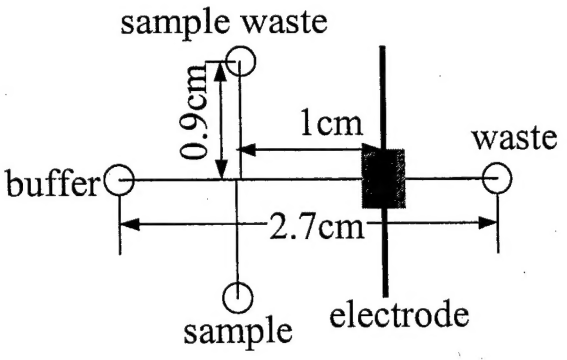
sample waste
0.9cm
1cm
waste
buffer
2.7cm
sample
electrode

b

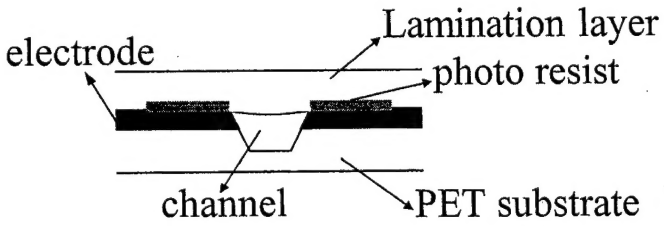
Lamination layer
electrode
photo resist
channel
PET substrate

Figure 2

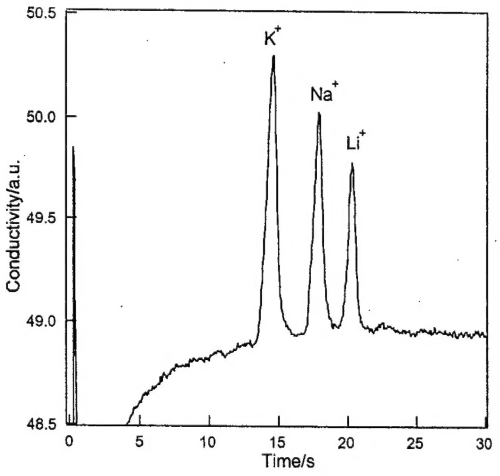
50.5
50.0
49.5
49.0
48.5
Conductivity/a.u.
K+
Na+
Li+
0
5
10
15
20
25
30
Time/s

Figure 3

a

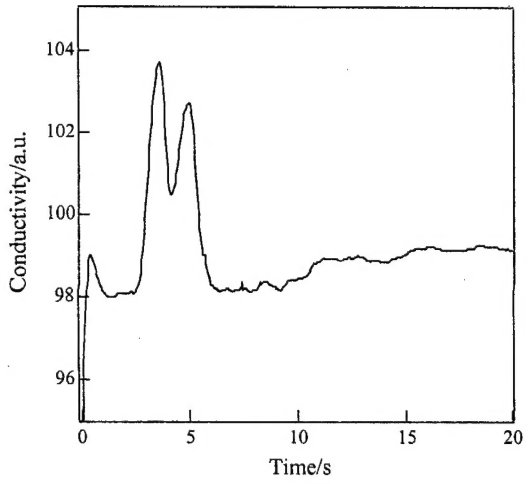
104
102
100
98
96
Conductivity/a.u.
0
5
10
15
20
Time/s

b

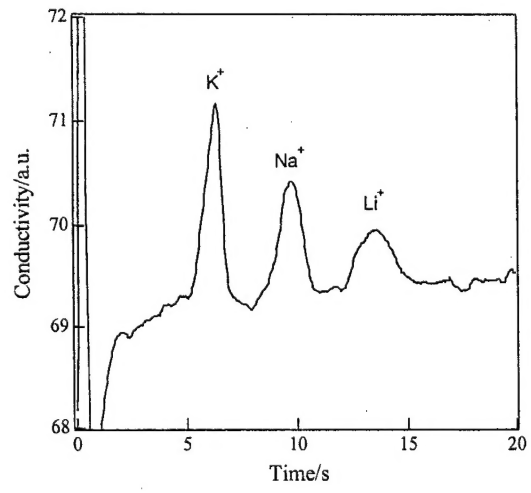
72
71
70
69
68
Conductivity/a.u.
K+
Na+
Li+
0
5
10
15
20
Time/s